Contents lists available at ScienceDirect

Chemical Engineering & Processing: Process Intensification

journal homepage: www.elsevier.com

Reverse flow reactors as sustainable devices for performing exothermic reactions: Applications and engineering aspects

Pablo Marín, Fernando V. Díez, Salvador Ordóñez*

Department of Chemical and Environmental Engineering, University of Oviedo, Facultad de Química, Julián Clavería 8, 33006, Oviedo, Spain

ARTICLE INFO

Keywords:
Dynamic reactor
Periodic operation
Catalytic reactor
Fixed-bed reactor
Integrated device
Regenerative oxidizer

ABSTRACT

Reverse flow reactors are fixed-bed reactors combining in a single intensified device chemical reaction and regenerative heat transfer (energy is stored in a bed as sensible heat). To accomplish this goal, reverse flow reactors are operated in a forced unsteady state created by periodically changing the flow direction. The most important applications of reverse flow reactor are reviewed: oxidation of hydrocarbons and sulphur dioxide, and selective catalytic reduction of nitrogen oxides. These applications involve exothermic reactions. However, recent developments have also made possible it possible the use of reverse flow reactors with endothermic reactions, such methane steam reforming.

The modelling of reverse flow reactors is addressed based on the models available for fixed-bed reactors. Practical considerations regarding reverse flow reactors are considered: the selection of the type of bed, the issues of the use of lab-scale devices at dynamic conditions, the assessment of autothermal operation and heat extraction and the integrated adsorption concept. The latter is an innovative concept based on the periodical adsorption in the bed of some of the reactants, products or other feed compounds. This mass regeneration can be combined with the heat regeneration capabilities of reverse flow reactors to increase the degree of process intensification.

Nomenclature

a	surface to bed volume ratioo m2/m3bed)
c_i	gas molar concentrationonmol/m3)
C_P	heat capacitytyJ/kg k
D_e	ed effective dispersion coefficient nt 2/s)
h	gas to solid heat transfer coefficientt W/m2 KK
k_e	bed effective thermal conductivitytyW/m K
K_C	gas-solid mass transfer coefficientntm/s/
L	reactor lengthh mm
m	mass flow ratee kg/ss
M_w	average molar weighthtkg/molo
Q	heatt WW)
r_i	reaction ratetemol/m3 s
t	timee ss
T	temperaturee KK
T_{ph}	pre-heating temperatureurK
t_{sw}	w switching tig ti
u	gas superficial velocityy m/ss
v	gass (interstitiaal) velocity (m/
y	mole fraction (-)
z	spatial coordinatee mm

Greek symbols

ΔH_R	heat of reaction
ΔT_{ad}	adiabatic temperature rise (ºC)
ε	bed porosity (-)
η_{th}	heat storage efficiency (-)
ρ	density (kg/m^3)
ω^T	velocity of the thermal front (m/s)

Subscripts

0	inlet
G	gas
ign	ignition
ph	pre-heating
r	reaction

* Corresponding author.
Email address: sordonez@uniovi.es (S. Ordóñez)

https://doi.org/10.1016/j.cep.2018.11.019
Received 19 September 2018; Received in revised form 19 November 2018; Accepted 25 November 2018
Available online xxx
0255-2701/

S	solid
St	storage

1. Introduction

Global warming, caused by the anthropogenic emissions of greenhouse gases, is one of the most important environmental concerns of the last decades. The efforts of the Governments to fight against greenhouse gas emissions have been focused in two strategies: increase of efficiency and replacement of energy sources by carbon-neutral ones (e.g. renewable sources, such as wind, solar, hydropower or biomass).

The increase of efficiency in industry has led to the development of new sustainable technologies and the improvement of the existing ones. Process intensification has played an important role. Heat transfer and recuperative systems have become an important tool to recuperate energy from, for example, effluent streams and transfer it upstream of the process. By implementation of these intensification measures, energy consumption at industrial scale can be reduced and, hence, the emission of greenhouse gases [1–4].

In this context, reverse flow reactors (RFR) are an important tool to improve the efficiency and sustainability of industrial processes. Reverse flow reactors are a type of fixed-bed reactor operated under forced unsteady state, created by means of periodic changes in the flow direction [5,6]. This produces temperature and concentration fronts that move back and forth through the bed. Consequently, reverse flow reactors are able to store heat, as sensible heat, in the bed packing, which increases considerably the thermal efficiency of the reactor [4].

The concept of RFR was originally introduced by Cottrell in 1935 [7] for the purification of gases. In the 1950s, the first application of catalytic flow reversal reactors appeared. However, the mayor application of this technology started in the 1970s thanks to the developments of the team of Prof. Matros in the Boreskov Institute of Catalyst (Novosibirsk, Russia) [5]. The first industrial-scale applications of reverse flow reactors consisted of the oxidation of sulphur dioxide and the combustion of volatile organic compounds emissions [8].

2. Working principle of reverse flow reactors

The basic elements of a RFR are a fixed-bed and a set of valves responsible for the change in the flow direction. The layout of a typical reverse flow reactor is depicted in Fig. 1. Alternatively, the valves can be replaced by a device where the whole reactor bed rotates to introduce the feed through different sections [9]. The fixed-bed can be made of one type of material or layers of different solids, such as catalyst, inert or adsorbent materials. A typical configuration for catalytic RFRs consists of a central catalytic bed and two inert beds at both sides. As shown in Fig. 1, the fixed-bed can be housed in more than one tower, connected by a central open chamber. This is particularly useful for non-catalytic reactions (e.g. a thermal combustion), where the open chamber provides enough residence time for the reaction.

In a reverse flow reactor, the different fixed-bed layers can play multiple roles: catalysis ofchemical reactions, storage of energy as sensible heat or storage of chemical species by adsorption. This multiple functionality determines the timing of the periodic change in the flow direction, as illustrated in the following paragraphs.

Consider an exothermic catalytic reaction (e.g. a catalytic combustion) carried out in a reverse flow reactor consisting in three sections: two inert, at the reactor ends, and one catalytic in the centre. First, to bring the unit online, the first section of the bed is pre-heated above the ignition temperature of the reaction mixture (this can be accomplished using a separate source of energy, such as an electric heater or a gas burner). This pre-heating is necessary only at the reactor start-up, unless the reactor extinguishes, which must be avoided.

When the bed reaches the operating temperature, the feed (usually at low temperature) is introduced into the unit. The sensible heat stored in the solid bed is now used to heat the gas. This creates a temperature front in the bed that moves in the gas flow direction, as shown in Fig. 2. When the gas temperature is above the ignition temperature, the reaction takes place in the catalytic bed (the reaction zone of the centre in Fig. 2). The heat released by the exothermic reaction causes a further increase in temperature of the reacting mixture.

Finally, the hot reacted gas feed reaches the third section of the bed, where the solids are cold. Hence, heat is transferred from the gas to the solid, and stored as sensible heat in the bed. This creates a second temperature front of decreasing temperature (Fig. 2, right inert bed).

The temperature fronts created in the bed determine the characteristic parabolic temperature profile of Fig. 2, with a more or less prominent temperature plateau in the middle of the bed. The fronts are not stagnant, both move in the direction of the gas flow. Therefore, the flow direction must be switched before the temperature of the first bed, and hence the temperature of the feed entering the catalytic bed is too low, which would produce the reactor extinction. Without the principle of reversal, the high temperature plateau within the reactor would migrate in the direction of the gas flow and eventually leave the catalytic bed and the reactor.

One of the key aspects in RFR is the regenerative heat transfer that takes place between the gas and the solids. As explained, heat is stored between cycles in the solid bed as sensible heat. Thus, while one side

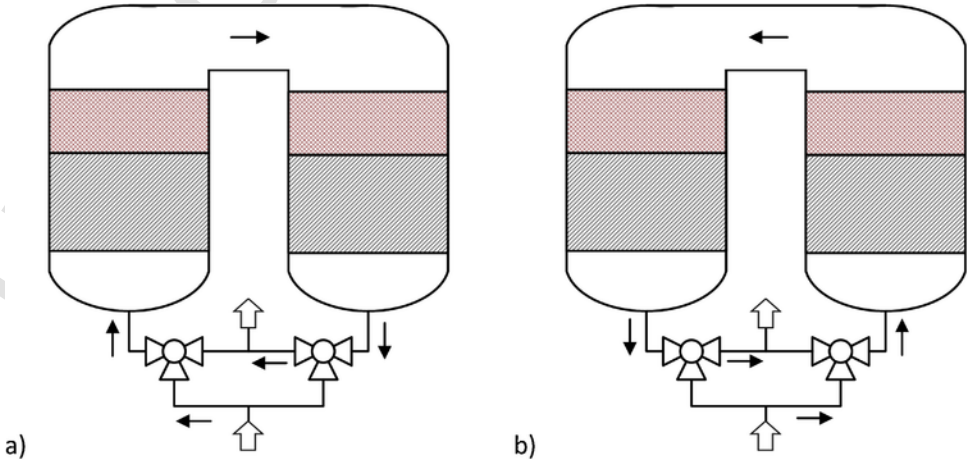

Fig. 1. Layout of a typical reverse flow reactor. Change of flow direction: a) direct flow and b) reverse flow.

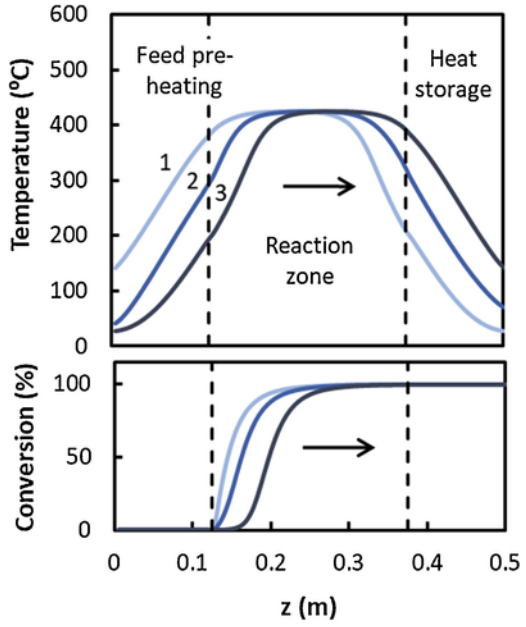

Fig. 2. Typical temperature and conversion profiles of a reverse flow reactor at the beginning of cycle (1), middle (2) and end (3). The dashed lines delimit the inert and catalyst beds. The arrow indicates the direction of the flow. Combustion of 1915 ppm methane (ΔT_{ad} = 53 °C) over a Pd-based monolith (superficial velocity 0.15 m/s, space velocity 1080 h^{-1} and switching time 300 s) [46].

of the reactor is used for heating the gas feed, the other side is being regenerated by the high temperature exhaust. When the flow direction is switched, the role of both beds is also switched.

Reverse flow reactors can also be used to create a forced un-steady state that results in improvements in the local reaction rate. For example, consider a chemical compound that adsorbs on the catalyst surface before reaction, the flow reversal can be used to control the catalyst surface coverage and, hence, improve reaction rate with respect to the steady state. In other situations, the flow reversal can help in the development of the desired dynamic concentration profiles, leading to higher selectivity. Thus, when some of the reactants or products adsorbs preferably on the reactor bed the reactor is actuating as a 'mass regenerators', instead of the 'heat regeneration' effect explained above [10–13].

Other dynamic reactors, based on the 'mass regeneration' effect in a similar way to reverse flow reactors, are the chromatographic reactors and simulated countercurrent moving-bed reactors [14,15].

3. Applications of reverse flow reactors

In this section, the different applications of reverse flow reactors, summarized in Table 1, are presented and discussed.

3.1. Oxidation of volatile organic compounds

Volatile organic compounds (VOCs) are a group of gaseous pollutants formed by many different types of compounds, such as hydrocarbons (e.g. propane, hexane, ethane, etc.), aromatics (e.g. benzene, toluene, naphthalene, etc.) and oxygenates (e.g. acetone, methanol, ethyl acetate, etc.). All of them have a low boiling point (less than 250 °C at 1 atm) and many of them cause photochemical smog when emitted to the atmosphere. At industrial scale, VOCs are generated in many sectors, such as oil refineries, chemical or pharmaceutical industries

Table 1
Summary of application of reverse flow reactors.

Process	Reaction	Degree of development	Advantages	References
Oxidation of volatile organic compounds (VOC)	VOC + O_2 → CO_2 + H_2O	Commercial	Autothermal/less energy consumption High conversion Low temperature combustion	See Table 2 for more details.
Oxidation of methane	CH_4 + 2 O_2 → CO_2 + 2 H_2O	Industrial demonstration	Autothermal/heat recovery	See Table 3 for more details.
Oxidation of sulphur dioxide	SO_2 + 0.5 O_2 ⇄ SO_3	Commercial	Autothermal High conversion Less pieces of equipment	[65,66,67,69,70,71,154,155]
Selective catalytic reduction of nitrogen oxides	NO + NH_3 + 0.25 O_2 → N_2 + 1.5 H_2O	Industrial demonstration	High conversion/no ammonia slip Smaller reactor	[10,76,77,78,79,80,82,156,157]
Synthesis of methanol	CO + 2 H_2 ⇄ CH_3OH	Simulation	High conversion	[85,86,87,88]
Synthesis of ammonia	N_2 + 3 H_2 ⇄ 2 NH_3	Simulation	High conversion	[89,90]
Water-gas-shift reaction	CO + H_2O ⇄ CO_2 + H_2	Simulation	High conversion Less pieces of equipment	[91]
Partial oxidation of methane	CH_4 + 0.5 O_2 → CO + 2 H_2	Laboratory demonstration	Autothermal/less energy consumption Less pieces of equipment	[92,93,94,95,96,97,98,99,101,102,103,104,105,106,107,108,109,110,111,112]
Methane reforming	CH_4 + H_2O ⇄ CO + 3 H_2	Laboratory demonstration		[94,100,115,116,117]
Claus reaction	H_2S + 0.5 SO_2 ⇄ 1.5 S + H_2O	Proposal		[118]
Oxidation of hydrogen sulphide	H_2S + 0.5 O_2 → S + H_2O	Proposal		[8]
Decomposition of nitrous oxide	N_2O → N_2 + 0.5 O_2	Simulation		[119,158]

and polymer manufacture and processing [16]. VOCs are harmful for both humans and the environment; therefore, the emission of these compounds is strictly regulated. As explained in the next chapter, usually methane is not classified as a VOC.

Among the different end-of-pipe treatment techniques proposed to abate VOCs emissions at industrial scale, so-called oxidizers or combustors are a popular alternative. Oxidizers consist of a destructive technique based on the complete oxidation of organic compounds to carbon dioxide. It is very common, especially for treating lean VOC emissions, to add an external fuel to the gas feed, which raises the reaction temperature and ensures complete combustion.

In order to reduce the consumption of external fuel, most oxidizers are equipped with a heat recovery device, capable of recovering part of the heat of the exhaust gas to pre-heat the feed. There are two types of oxidizers according to the heat recovery devices used [17]: recuperative and regenerative. Recuperative oxidizers use a heat exchanger, where heat transfer takes place through a wall that separates the hot exhaust and the cold feed. These devices can operate in steady-state, and their heat storage efficiency is usually below 70%.

Regenerative oxidizers use packed-beds to store, as sensible heat, the energy of the hot exhaust gas; then, this energy is used to pre-heat the cold feed. Hence, operation of regenerative oxidizers is cyclic (forced unsteady state). Regenerative oxidizers are actually reverse flow reactors used for combustion reactions. In these devices, heat storage efficiency increases to 90–95%, thanks to the efficient direct gas-to-solid heat transfer [18,19].

There are two types of regenerative oxidizers: thermal and catalytic. Thermal regenerative oxidizers (RTO) do not use catalysts and rely only on homogeneous combustion reactions. These oxidizers are typically equipped with an open chamber, placed between the two regenerative beds, where flame combustion takes place at high temperature (if needed, supplementary fuel is added to this chamber). Catalytic regenerative oxidizers (RCO) use a catalyst to reduce the ignition temperature, which decreases combustion temperature and the requirement of supplementary fuel. For this reason, RCOs usually exhibit a higher heat storage efficiency than RTOs. Typical RCOs consist of a catalytic bed, placed in the middle of two inert beds; all the beds can store heat, but the heat regeneration capacity is concentrated in the inert beds.

Table 2 summarizes the most recent scientific works of application of regenerative catalytic oxidizers, i.e. catalytic RFR, to the abatement of VOCs. For brevity, only the works based on experiments are considered. It is worth to point out the great variety of VOCs considered, including aliphatic (propane, butane, hexane) [5,20,21], olephinic (ethylene) [20,22,23] aromatic (benzene, toluene, xylene, naphthalene) [18,21,24–27] or oxygenated compounds (isopropyl alcohol, methyl ethyl ketone) [18,28,29], all of them emitted to the atmosphere in oil refineries, petrochemical, chemical or pharmaceutical plants, in process exhausts or due to the use of these compounds as solvents.

The catalysts considered in the oxidation of these VOCs can be classified into precious metal and metal oxide catalysts [30]. The most common precious metal active phases are Pd [5,31,32], and specially Pt [20–23]. Pd is recommended for short chain hydrocarbons (e.g. methane, ethane), while Pt is more active for larger molecules [16,33]. For some applications, a mixture of Pd and Pt is used. Regarding metal oxide catalysts, Cu with Co or Cr has been used in RCO for the oxidation of isopropyl alcohol, propane and butane [5,28,29].

Regarding the concentrations of the experiments of Table 2, the range is broad within 75–8500 ppm (0.0075-0.85%). However, there is no point in comparing different VOCs according to their concentration (in ppm). These compounds have may have a very different heat of combustion and, hence, the thermal performance of the oxidizer (e.g. the catalytic RFR) will vary a lot. In order to compare different compounds, it is recommended the use of the adiabatic temperature rise, defined as the increase in temperature produced by an exothermic reaction conducted until complete conversion at adiabatic conditions.

$$\Delta T_{ad} = \frac{\left(-\Delta H_R\right) y_0}{C_{PG} M_w}$$

Where ΔH_R is the enthalpy of reaction, y_0 is the feed mole fraction, C_{PG} is the heat capacity of the reacting mixture and M_w is average molar weight.

Some of the authors [20,21,27] also studied the influence of mixtures of volatile organic compounds on the reactor performance. Thus, in these cases, to ensure complete combustion, the reactor should be pre-heated to a temperature above the highest ignition temperature of the compounds of the mixture. Otherwise, for the case of compounds of very different ignition temperature, it is possible to have complete combustion of only one compound; the heat released in the reactor being unable to increase temperature above the ignition temperature of the other compound. Other studies addressed the decrease in perfor-

Table 2
Summary of works on VOC catalytic combustion in reverse flow reactors.

Catalyst	Bed type	Catalytic bed size	Compound	Concentration	t_{sw} (s)	u_0 (m/s)	Year	References
Dolomite	Spheres 1-3 mm		1-methyl naphthalene	2400 ppm	–	0.02-0.05	2014	[26]
Pt/Al_2O_3	Spheres 4 mm	1.1 dm^3	Benzene Methane	ΔT_{ad} = 28-70 °C	360-600	0.2-0.8	2011	[27]
Cu/MolSieve	Spheres 3 mm	5.6 dm^3	Isopropyl alcohol	200-400 ppm	120-300	0.37-0.74	2010	[29]
Pt/Al_2O_3	Spheres 3 mm	0.25 dm^3	Toluene Hexane	190-390 ppm 180-365 ppm	300-600	0.15	2008	[21]
Pt/Al_2O_3	Spheres 3 mm	0.79 dm^3	Ethylene	5000-8500 ppm	–	0.5-0.73	2008	[23]
Cu-Co/ monolith	Monolith	45 dm^3	Isopropyl alcohol	200-400 ppm	120	0.34-0.74	2008	[28]
–	Particles 11 mm	42 dm^3	N, N-dimethyl formamide	300-750 ppm	90	0.39	2007	[159]
Monolith	Monolith	1.5 dm^3	Xylene	95-320 ppm	16	1.2	2005	[25]
Pt/Al_2O_3	Spheres 1.6 mm	0.35 dm^3	Ethylene	500-5000 ppm		0.15-0.30	2003	[22]
Monolith	Monolith	1.5 dm^3	Xylene	130-290 ppm	10-20	3	2001	[24]
Monolith	Monolith Granite gravel	0.15 dm^3	Methyl ethyl ketone Toluene	120-300 ppm 75-185 ppm	135	0.23	2000	[18]
Pd-monoith	Monolith	4.7 dm^3	Gas turbine exhaust			1.3-2.6	2001	[31,32]
Pt/Al_2O_3	Spheres 4.5 mm	10.7 dm^3	Ethene Propane	450-1800 ppm 260-1050 ppm	200-1600	0.4	1997	[20,160,161]
Cu-Cr	Rings 15-25 mm	12-50 dm^3	Butane Propane	500-1400 ppm 450-1300 ppm	15-90	0.42-0.75	1984	[5]
Pd-monolith	Monolith	0.7 dm^3	Propane Methane	700-1400 ppm	60-120		1988	[5]

mance that occurs when the VOC adsorbs at the entrance of the bed [34].

3.2. Oxidation of methane

Methane, though is a gaseous organic compound, usually is not classified as VOC, because it is nontoxic and does not contribute to the formation of photochemical smog. However, methane is a powerful greenhouse gas with a global warming potential (GWP) of 28 (e.g. 1 kg of methane produces a radiative forcing over a period of 100 years equivalent to the emission of 28 kg of carbon dioxide), so its emissions are affected by global warming regulations [35].

Methane anthropogenic emissions are mainly generated in coal mines, landfills, gas processing and distribution systems, waste and water treatment plants, etc. The concentration of methane in these emissions can be very different, but it is critical to implement treatment or valorisation processes [36–38].

Form the environmental point of view, one possibility for reducing the net impact of methane is its oxidation to carbon dioxide. The stoichiometric equation is:

$$CH_4 + 2\,O_2 \rightarrow CO_2 + 2\,H_2O$$

This way, the radiative forcing over a period of 100 years caused by the methane emission would be reduced by a factor of 28, i.e. the GWP (note that the GWP accounts for the radiative forcing caused only by the methane molecule rather than the carbon dioxide eventually generated from methane in the atmosphere) [35]. The transformation of methane into carbon dioxide, may seem not to be the best option for reducing greenhouse gas emissions, but in fact it is a great improvement in terms of net radiative forcing. Additionally, in many cases this is the only abatement process available in practice.

In addition to this, the high heat of combustion of methane (39.8 MJ/m^3) makes attractive the recuperation of this energy, or at least part of it, as heat or even electricity. In this context, the use of gas turbines offers the advantage of a direct electricity generation. However, a minimum concentration of methane in the range 1–2% vol. is required [39]. For lower concentrations, recuperative or regenerative combustion techniques are preferred [37].

So, regenerative oxidizers represent a good alternative to turbines for the case of lean methane emissions. Thanks to the regenerative heat transfer, these devices exhibit a high thermal efficiency (90–95%). This means that autothermal operation, i.e. without addition of external heat or fuel, is possible, even for very low methane concentrations. As methane is non-toxic, low concentrations of methane are allowed in the exit emissions.

In the same way to the combustion of VOCs, there are two types of regenerative oxidizers for the combustion of methane, thermal and catalytic. Methane oxidation in catalytic RFR (or RCO) has been studied experimentally by many authors. One of the reasons of this interest is because methane is one of the hydrocarbons most refractory towards oxidation, thus requiring a higher ignition temperature [40]. This means that a successful operation of the reactor with methane will be easily extended to most VOCs without the need of long individual studies.

The scope of the research on methane catalytic oxidation in RFR has been varied: experiments of proof of concept aimed at demonstrating the technical feasibility for a given situation, the elucidation of the influence of the main operating parameters and bed types and shapes, the gathering of experimental data to validate mathematical models, the testing of control and heat withdrawal systems, etc. Table 3 summarizes the most important works, which will be discussed in the following paragraphs.

As shown in Table 3, different types of catalysts have been studied in RFR, being Pd the most popular [41–48], the main reason being that

Table 3
Summary of works on methane catalytic combustion in reverse flow reactors.

Catalyst	Bed type	Catalytic bed size	Concentration	t_{sw} (s)	u_0 (m/s)	Study	Year	References
Pt/monolith	Monolith	3.3 dm^3	0.2%	600-1800	0.24	Influence of operation and humidity.	2017	[41]
Cu-Mn-Ce/Al_2O_3	Pellets	225 kg 1800 dm^3	0.2-1%	300-600	0.20	Pilot-scale. Testing of control and hot gas withdrawal.	2017	[55]
Cu-Mn/Al_2O_3	Spheres 4 mm	0.4 dm^3	0.4-0.45%	200-400	0.15	Integrated adsorption, H_2S	2016	[36]
Pd/monolith	Monolith 390 cpsi	0.3 dm^3	0.18-0.72%	100-600	0.15	Inhibition caused by water. Integrated adsorption, water	2015	[43] [152]
Pd/Al_2O_3	Monolith 400 cpsi	0.5 dm^3	0.3-0.5%	60-180	0.56	Heat withdrawal with a central heat exchanger.	2014	[42]
Pd/β-SiC	Foam 7 ppi	0.5 dm^3	0.27-0.54%	50-900	0.25-1.5	Model validation for ceramic foam supports.	2013	[44]
Pd/Al_2O_3	Spheres 3-5 mm	1.13 dm^3	0.4%	600	0.16	Periodic variation of inlet concentration.	2011	[45]
Pd/Al_2O_3	Spheres 3-5 mm	1.13 dm^3	mixture	360-600	0.2-0.8	Mixtures of benzene and methane.	2011	[27]
Pd/Al_2O_3	Spheres 2-3 mm	1.6 dm^3	0.3-0.5%	900-1800	0.2-0.3	Parameter study.	2010	[132]
Pd/monolith	Monolith 370 cpsi	0.5 dm^3	0.10-0.55%	180-900	0.15-0.3	Model validation for monolith supports. Testing of control system.	2010	[46,162]
–	Pellets Monolith			15-30		Thermal regenerative oxidizer.	2008	[131]
Non-noble metal	Rings 7.5 mm	12.5 dm^3	0.2-0.6%	100	0.7-1.2	Bed properties. Heat withdrawal.	2005	[56,57]
Pd/Al_2O_3 Cu-Mn/Al_2O_3	Spheres 3-4 mm	0.5 dm^3	0.35-0.45%	150-600	0.15	Control system. Catalyst properties.	2005	[47,133]
Non-noble metal	Rings 7.5 mm	12.5 dm^3	0.3-0.85%		0.15-0.65	Model validation. Heat withdrawal.	2000	[58,163]
–	Saddels		0.23-0.32%	90	0.53-1.1	Regenerative thermal oxidizer. Pilot-scale.	1997	[137]
Pd/Al_2O_3		0.7 dm^3	1.38-1.8%	34-104 min	0.28-0.5		1994	[48]
Cu-Cr	Rings 15-25 mm	130 dm^3	0.45-1.2%	130-200 min	0.4-0.6		1988	[5]

Pd provides higher activity [49]. Kinetic studies on Pd-based catalysts showed a 0.5–1.0-order dependence for lower alkanes, whereas a very weak or zero-order dependence was observed for oxygen [50–53]. It is now believed that the Mars and van Krevelen (redox) mechanism plays a role in methane combustion on Pd catalysts. According to this mechanism, the first step involves the reduction of PdO with methane, followed by a second step in which Pd is re-oxidized to PdO by oxygen [52,54].

Other catalysts used in the studies are metal oxides, e.g. Cu, Mn or Cr oxides [5,36,47,55]. The main advantage of these catalysts is their lower cost, though the operating temperature must be increased to overcome their lower activity. The increase in temperature is from 350 to 400 °C of precious-metal catalysts to 500 °C for metal oxides. As a result, heat storage efficiency also suffers a small decrease.

The catalysts have been studied in the shape of random particles (i.e. spheres, rings, pellets, etc.) or structured packings (i.e. monoliths and ceramic foams). Each one offers both advantages and disadvantages, as explained in chapter 5.1.

The range of concentrations studied is 0.10 to 1% methane (Table 3). Autothermal operation for the lower boundary of the range is only attainable by the more active precious-metal catalysts. The higher boundary of the range corresponds to studies where the heat extraction from the reactor was tested [42,55–58]. This topic will be discussed in a separate section.

The superficial velocity in the experiments has been maintained between 0.15 and 1 m/s (Table 3). This parameter is linked to reactor size and pressure drop. Thus, a low superficial velocity results in low pressure drop, but the resulting reactor bed has a low length-to-diameter ratio. At industrial scale, a superficial velocity between 1 and 2 m/s (this depends of the type of bed, i.e. formed by random particles or monolithic blocks) is usually recommended to reduce the overall cost of the reactor [59].

The maximum switching time that can be used in RFRs depends on the superficial velocity, the bed length and properties (thermal inertia), as sketched in section 3. Therefore, the range of switching times is quite wide, from 15 to 60 s to 900–1800 s.

Regenerative thermal oxidizers, i.e. reverse flow reactors without catalyst for high-temperature homogenous gas phase reactions, have also been applied to methane oxidation at lean conditions [60–64].

3.3. Oxidation of sulphur dioxide

The oxidation of sulphur dioxide to sulphur trioxide is a reversible exothermic reaction, carried out at industrial scale in fixed-bed adiabatic reactors in series. In order to get high conversion avoiding equilibrium limitations, interstage cooling is used. The characteristic parabolic temperature profile that RFR develop spontaneously when operated with exothermic reactions and low-temperature feeding is very interesting for reversible exothermic reactions. Thus, when the feed enters the reactor, is heated gradually, and temperature increases to a maximum due to the heat released by the reaction. This increase in temperature results in high rate of reaction, before equilibrium is reached. Then, in the second half of the reactor, the bed is at a gradually lower temperature, which contributes to increase the equilibrium conversion.

The technology was patented by the Boreskov Institute of Catalyst [5] and was deployed at industrial-scale for processing low-concentration gases (1–5% SO_2) in nonferrous metallurgy. The process was studied experimentally and by means of simulations to understand the dynamics of the process [65–68]. Different reactor configurations were proposed [5]: adiabatic operation, with intermediate heat exchangers to extract the excess heat (concentrations higher than 2–3% SO_2), or the use of intermediate unidirectional beds. A combined control system of cycling and cooling was studied in an industrial-scale reverse flow reactor with two intermediate heat exchangers [69–71]. Most recently, solutions to deal with carbon monoxide/sulphur dioxide mixtures have been proposed [72].

3.4. Selective catalytic reduction of nitrogen oxides

Nitrogen oxides are an important environmental pollutant, mainly generated in combustion systems (e.g. power plants, motor vehicles, etc.), but also in the chemical industry (nitric acid production). The most widely used treatment technique is the selective catalytic reduction with ammonia, with overall reaction:

$$NO + NH_3 + 0.25\ O_2 \rightarrow N_2 + 1.5\ H_2O$$

Catalysts used for this process include noble metals, metal oxides and zeolites [73–75]. One of the most widely used at industrial-scale is vanadium oxide promoted by WO_3 (or MoO_3) and supported on titania (anatase). Honeycomb is the most common catalyst shape, providing low pressure drop, and good thermal and mechanical properties. In this reaction, ammonia is adsorbed on the catalyst surface; however, one of the problems of conventional reactors is the emission of unreacted ammonia when nitrogen oxide concentration fluctuates (the so-called ammonia slip). This important drawback should be avoided, since ammonia is also an important environmental pollutant.

Reverse flow reactors offer important advantages in this context. In this case, the flow reversal allows the trapping of ammonia by adsorption on the solid between cycles, preventing the ammonia slip. To accomplish this goal, the reactor is divided into two beds and ammonia is fed in between. This way, the reactor acts as a "mass regenerator", where any accidental excess of ammonia can be stored between cycles to be used when nitrogen oxide concentration increases. This behaviour is illustrated in Fig. 3, where the evolution with time of concentration profiles is depicted. As observed, nitrogen oxide is completely abated, while ammonia is kept within the reactor thanks to the flow reversal. In addition, the concentration of adsorbed ammonia in the reaction zone exhibits a boost with respect to conventional direct flow. As a consequence, reaction rate increases and the size of the reactor for a given conversion decreases [10].

The use of RFR for the selective catalytic reduction of nitrogen oxides was proposed by Agar and Ruppel [76] and Matros research group [5]. They used simulations to study and optimize the process, finding that ammonia feeding in the middle of the reactor is more efficient [77]. They also studied the system on pilot plant, and implemented it on a Russian oleum plant [78]. The experimental work regarding this reaction was recently completed by means of an experimentally validated model [10].

Other simulation studies were focused on the influence of ammonia feed concentration and switching time on the concentration profiles in the reactor [79–81]. The performance of RFR was compared to that of reactors network (a system composed of several fixed bed units, the feed switching periodically among them) [82–84].

3.5. Other applications

The abovementioned applications of reverse flow reactors are the most studied ones, and applied at industrial-scale. However, as summarized in Table 1, many other applications have been proposed.

The successful application of RFR to the oxidation of sulphur dioxide has motivated the applications to other equilibrium-limited reversible exothermic reactions. Among them, the synthesis of methanol [85–88], ammonia [89,90] and the water-gas-shift reaction [91] are the most remarkable. In these processes, the equilibrium limits conversion in conventional adiabatic reactors. The use of reverse flow reac-

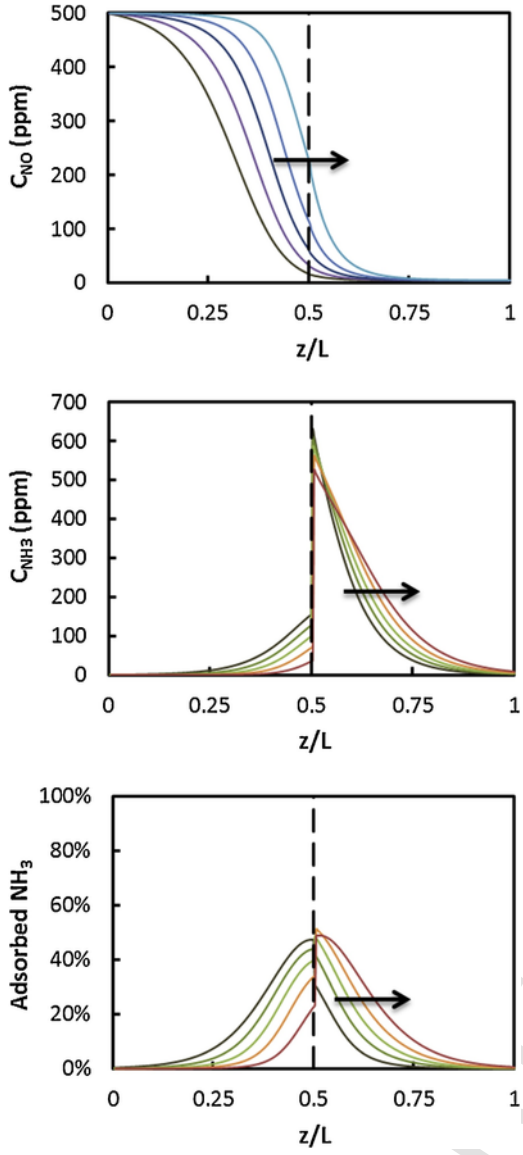

Fig. 3. Reverse flow reactor for the selective catalytic reduction of nitrogen oxides: evolution of concentration profiles during a half-cycle (300 s). The arrow indicates the flow direction and the dashed line the point where ammonia is introduced [10].

tors, with their characteristic temperature profile and with low-temperature feeding, makes it possible to increase the conversion at the end of the reactor, where temperature decreases.

Methane partial oxidation and autothermal/steam reforming to synthesis gas have also been studied in reverse flow reactors. The main advantage is the possibility of autothermal operation in robust and compact devices, with a decrease in investment and operating costs [92–114]. The methane reforming reaction can be carried out with oxygen (exothermic) or in the absence of oxygen (endothermic). In the latter case, an exothermic reaction (e.g. combustion) is coupled with the reforming reaction through the reverse flow reaction cycling [115–117].

In addition to the previous examples, RFR has also been proposed as a good alternative in the Claus process (synthesis of sulphur from hydrogen sulphide and sulphur dioxide) and hydrogen sulphide oxidation [8,118].

Also some other environmental applications have been considered, such as the decomposition of nitrous oxide [119].

4. Modelling of reverse flow reactors

4.1. Dynamic models for reverse flow reactors

Reactor modelling and simulation is today an important tool for the design and optimization of chemical reactors. Reverse flow reactors are a type of fixed-bed reactor operated in unsteady state, so dynamic models suitable for fixed-beds should also be considered for reverse flow reactors.

The modelling of fixed-bed reactors is actually a multi-scale task ranging from the catalyst-molecule interactions in the nano-scale to the flow of fluids in the macro-scale. On increasing the number of scales included in the model, its complexity increases. Such complex models can be required in some cases, but most commonly, the models can be simplified according to the degree of description and accuracy demanded by a given application (e.g. reactor design, optimization, dynamic modelling, etc.). The reactor or macro-scale comprises the phenomena taking place in the reactor bed, e.g. mass and heat transfer, reaction, fluid flow, etc. The reactor bed can be modelled in 3D, but more commonly, due to symmetry, important gradients are only expected in some coordinates. Thus, simplified 1D and 2D models are very common [120–122].

For the case of reverse flow reactors, continuous dynamic models are the most popular [72,123–125], providing accurate results for the tasks of reactor design, optimization and dynamic simulation. The bed in reverse flow reactors is usually of large diameter and behaves close to adiabatic conditions. For this reason, the velocity profile is almost flat, and due to the adiabatic conditions, temperature and concentration radial gradients can be neglected. Thus, models in 1D geometry that solve gradients in the axial coordinate are enough to describe the reactor.

Table 4 shows the continuum heterogeneous model in 1D suitable to simulate reverse flow reactors. This model is formed by the mass and heat balance equations, which for heterogeneous models are applied separately to the gas and solid phases. Heterogeneous models are recommended for reactions that are fast and with a high released/absorption of heat, i.e. when important concentration and temperature differences between the solid and gas phase are expected. This is actually the case in most reverse flow reactors, particularly the oxidizers and, for this reason, this heterogeneous models are the most commonly used [126].

The meaning of the different terms of the equations is indicated in the table: accumulation, convection, dispersion, phase transfer and reaction. The mass dispersion term is used to model deviations from the ideal plug flow and to account for mixing in the axial direction. The magnitude of this term depends of the type of packed bed, being more important in beds made of random particles than in monolithic beds. For the case of honeycomb monoliths, heat dispersion in the solid heat balance accounts for axial conduction inside the solid. To solve the model, parameters dependent of the type of bed, in this case, mass and heat dispersion (D_e and k_e) and transfer coefficients (K_C and h) are needed. The accuracy of these parameters is crucial for the success of the simulation, so empirical correlations suitable for the type of bed and flow pattern (e.g. random particle, monolithic or foam packed beds) are required [44]. In addition, a reaction rate expression is required to evaluate reaction terms. Here, both gas and solid-catalysed reactions are considered in the general model of Table 4, though in many situations only one of them is important, e.g. the homogeneous gas-phase reaction in thermal oxidizers and the solid-catalysed in low temperature catalytic oxidations.

Table 4
Continuum lumped heterogeneous model used for reverse flow reactors.

Mass and heat balances for heterogeneous models				
Accumulation	Convection	Dispersion	Phase transfer	Reaction
$\frac{\partial c_{Gi}}{\partial t} =$	$-v_G \frac{\partial c_{Gi}}{\partial z}$	$+D_{Ge} \frac{\partial^2 c_{Gi}}{\partial z^2}$	$+\frac{K_C a}{\varepsilon}(c_{Si} - c_{Gi})$	$+ r_{Gi}$
$\frac{\partial c_{Si}}{\partial t} =$			$+\frac{K_C a}{\varepsilon}(c_{Gi} - c_{Si})$	$+\frac{(1-\varepsilon)}{\varepsilon} r_{Si}$
$\rho_G C_{PG} \frac{\partial T_G}{\partial t} =$	$-\rho_G C_{PG} v_G \frac{\partial T_G}{\partial z}$	$+k_{Ge} \frac{\partial^2 T_G}{\partial z^2}$	$+\frac{ha}{\varepsilon}(T_S - T_G)$	$+\sum_j r_{Gj}(-\Delta H_{Rj})$
$\rho_S C_{PS} \frac{\partial T_S}{\partial t} =$		$+k_{Se} \frac{\partial^2 T_S}{\partial z^2}$	$+\frac{ha}{1-\varepsilon}(T_G - T_S)$	$+\sum_j r_{Sj}(-\Delta H_{Rj})$
Boundary conditions				
Direct flow:	$v_G = v_{G0}\rho_{G0}/\rho_G$	Reverse flow:	$v_G = - v_{G0}\rho_{G0}/\rho_G$	
$z = 0$	$z = L$	$z = 0$	$z = L$	
$c_{Gi} = c_0$	$\frac{\partial c_{Gi}}{\partial z} = \frac{\partial T_G}{\partial z} = 0$	$\frac{\partial c_{Gi}}{\partial z} = \frac{\partial T_G}{\partial z} = 0$	$c_{Gi} = c_0$	
$T_G = T_0$	$\frac{\partial T_S}{\partial z} = 0$	$\frac{\partial T_S}{\partial z} = 0$	$T_G = T_0$	
$\frac{\partial T_S}{\partial z} = 0$			$\frac{\partial T_S}{\partial z} = 0$	
Initial conditions				
$c_{Gi} = c_{Si} = 0$	$T_G = T_S = T_{ph}$			

4.2. Propagation of thermal fronts

The velocity of the temperature fronts that travel through the reactor bed can be derived from the energy balance equations. In the absence of reaction, the velocity of the thermal front can be determined as the ratio of convection and accumulation terms [127]:

$$\omega^T = \frac{\varepsilon \rho_G C_{PG} v_G}{\rho C_P} \simeq \frac{\varepsilon \rho_G C_{PG} v_G}{(1-\varepsilon)\rho_S C_{PS}}$$

As shown, the velocity of the thermal front is proportional to the gas velocity and the ratio of thermal inertias of the gas and bed. The average thermal inertia of the bed is approximated by that of the solid, $\rho C_P \approx (1 - \varepsilon)\rho_S C_{PS}$, since solid density is much higher than gas density.

Considering the physical properties of the materials typically used in reverse flow reactors (e.g. the gas is air and the solids are ceramics), the velocity of the thermal front can be estimated within the range:

$\omega^T = v_G/(150–7500)$, typically $\omega^T = v_G/3500$

Hence, the velocity of the thermal front is much lower than the velocity of the gas flow. This characteristic of the regenerative heat transfer makes possible the use in practice of reverse flow reactors, as it allows high switching times.

The presence of an exothermic chemical reaction modifies the velocity of thermal fronts, due to the heat released by the reaction. This is accounted for by means of an energy balance [127]:

$$\omega^R = \left(1 - \frac{\Delta T_{ad}}{\Delta T}\right) \omega^T$$

The adiabatic temperature rise, $\Delta T_{ad} = (-\Delta H_R) y_0 / M_w C_{PG}$, depends on the heat of reaction and is proportional to the feed concentration. The temperature rise of the front can be split into two contributions, $\Delta T = \Delta T_{ign} + \Delta T_{ad}$. The ignition temperature rise, $\Delta T_{ign} = T_{ign} - T_0$, is the minimum temperature required above the feed temperature T_0 to start the reaction. This factor depends of the reactant-catalyst system. Considering the definitions of these factors, the velocity of a reaction front can be calculated using the following expression:

$$\omega^R = \frac{\omega^T}{\left(1 + \frac{\Delta T_{ad}}{\Delta T_{ign}}\right)}$$

According to this equation, $\omega^R \leq \omega^T$. This means that the heat released in the reaction decreases the velocity of the temperature front.

For the case of $\Delta T_{ign} \gg \Delta T_{ad}$, the reaction front can be approximated by a thermal front, $\omega^R \simeq \omega^T$. As an example, this situation corresponds to the thermal (non-catalytic) oxidation of 0.18% methane in air ($\Delta T_{ad} = 50$ °C). The non-catalytic oxidation of methane requires a considerably high ignition temperature, ΔT_{ign} of at least 900 °C (i.e. $\Delta T_{ign} = 18\,\Delta T_{ad}$) [128]. The velocity of the reaction front is calculated as $\omega^R = 0.95\,\omega^T$. On the contrary, the catalytic oxidation of 368 ppm of toluene ($\Delta T_{ad} = 50$ °C) on a Pt/Al_2O_3 catalyst requires an ignition temperature of 166 °C (i.e. $\Delta T_{ign} = 2.8\,\Delta T_{ad}$) [40]. For this case, the velocity of the reaction front is much different from the thermal front, $\omega^R = 0.74\,\omega^T$.

It is very common to replace part of the catalyst bed by inert materials at both sides of the reactor. This has an influence in the front traveling along the bed. In the inert beds, temperature fronts are purely thermal (unless temperature increases above the non-catalytic ignition temperature, which is uncommon), but in the catalytic bed, a reaction front can develop. Frequently, the feed is heated well above the ignition temperature in the inlet inert bed, so that the reaction starts suddenly when the feed reaches the catalytic bed. As a result, most of the reaction heat is released in a short portion of the bed, distorting the shape of the temperature front.

4.3. Gradients inside the solid

The model presented in Table 4 does not consider the presence of gradients inside the solid (i.e. for beds made of random particles, intraparticle gradients). However, in reverse flow reactors, with energy being stored as sensible heat inside the solid, temperature of the solid surface may differ from that of the centre. This is not accounted for in the model of Table 4, where it is assumed that heat is transferred very fast inside the solid (isothermal local solid). To evaluate, if this assumption is valid for reverse flow reactors, the heat balance equation for the solid phase can be used:

$$\frac{\partial T_S}{\partial t} = \alpha \nabla^2 T_S \qquad \begin{matrix} \nabla T_S|_{symmetry} = 0 \\ T_S|_{surface} = T_G \end{matrix}$$

For simplicity, the reaction term is not considered (valid only for thermal regenerator beds). Considering typical properties of solids used as regenerative beds ($\rho_S = 2300\ \mathrm{kg/m^3}$, $C_{PS} = 900\ \mathrm{J/kg\ K}$ and $k_S = 1.5\ \mathrm{W/m\ K}$), $\alpha = k_S/\rho_S C_{PS} = 7.25 \cdot 10^{-7}\ \mathrm{m^2/s}$.

For the case of monolithic beds, the equation is solved in rectangular coordinates, for which the condition of almost no temperature dif-

ference, i.e. $T_S|_{surface} - T_S|_{symmetry} < 0.9$, is met for $\alpha t/b^2 > 1$ [129]. Considering a typical monolith geometry (wall thickness of 0.4 mm, $b = 0.2{\cdot}10^{-3}$ m, and bed porosity of 75% [130]), the time required to heat up (or cold down) the inside of the solid is $t = b^2/\alpha = 0.055$ s. During this time and for a superficial gas velocity of 1 m/s, the thermal front may have travelled 0.04 mm of the bed length (thermal front velocity $8{\cdot}10^{-4}$ m/s).

For the case of random particle beds made of spherical particles, the equation must be solved in spherical coordinates. Thus, the condition of almost no temperature difference is now met for $\alpha t/R^2 > 0.3$ [129]. As before, for typical bed geometry (particle diameter of 6 mm and bed porosity of 40%), the time required for heat transfer is 3.7 s, which is traduced into 0.7 mm of bed length travelled by the thermal front (thermal front velocity $1.8{\cdot}10^{-4}$ m/s).

According to these calculations, typical solid materials used in reverse flow reactors (of both monolithic and random particle geometries) can be considered quasi-isothermal. This means that heat is transferred from the surface to the inside of the solid very fast (in 0.055 and 3.7 s, respectively, for monolithic and random particle beds). In this period of time, the thermal front has travelled only a short distance, 0.04 and 0.7 mm, respectively, for monolithic and random particle beds. Therefore, the influence of temperature gradients inside the solid on the overall performance of reverse flow reactors can be considered negligible compared to other phenomena. For this reason, as a general recommendation, the solving the model equation in the particle scale to obtain the solid internal gradient is not required.

5. Practical considerations

5.1. Type of bed packing

An important aspect to be considered in RFR design is the type of bed packing. The three most common types of bed packing available for fixed-bed reactors are random particles, honeycomb monoliths and foams. Traditional catalytic beds consist of random particles, such as spheres, rings, or pellets. These particles usually are porous with a high internal surface area that allows high dispersion of the catalytic active phase. Structured beds, made of honeycomb monoliths, and ceramic foams, have been proposed and tested for reverse flow reactors [42–44,46,131]. Honeycomb monoliths are blocks formed by parallel channels that allow the gas flow with very low pressure drop. The active phase is deposited in a porous washcoat layer that covers the walls of the channels. Ceramic foams are a relatively new catalyst support made of a reticulated three-dimensional structure that holds a network of macroscopic interconnected cavities. These supports offer higher fluid-to-solid transport capabilities than honeycomb monoliths with low pressure drop.

As mentioned, structured beds offer lower pressure drop, though, the thermal inertia of the bed is usually reduced [44]. To overcome this issue, the material of the bed should be carefully selected (e.g. type of refractory ceramics, porosity, etc.) and sized (e.g. nominal size of the structure, bed length, etc.). As an example, monolithic beds of large channel size and high porosity present lower thermal inertia, which must be compensated with an increase in bed length to achieve the same performance.

5.2. Reactor size: laboratory versus industrial scale

Bed sizes covered in published studies (Table 2 and 3) range from lab-scale devices (0.3-10 dm^3) to large-scale ones (130-1800 dm^3). Lab-scale reverse flow reactors have been useful in the determination of the relationships between the main operating variables, such as gas velocity, switching time, feed concentration, pre-heating temperature, bed size, etc. [44,46,132,133]. At small-scale, it is easier to make changes in these and other variables with low costs and risks to the reactor integrity. However, small-scale adiabatic reactors operated in unsteady state present the drawback of the influence of the thermal insulation on the thermal inertia of the reactor and, hence, on the reactor dynamics, e.g. the evolution of temperature profiles with time. In large-scale reactors, the insulation affects only a relatively small portion of the bed close to the wall.

Some authors have proposed special designs for lab-scale devices aimed to decrease the influence of the insulation thermal inertia, and then approach the dynamics of large adiabatic reactors. The device depicted in Fig. 4 is formed by a multi-section electric oven, capable of heating and cooling independently each section [134–136]. The working principle of this oven consists on measuring the temperature of the inside of the reactor continuously and setting this temperature dynamically in the section that surrounds the reactor. Thus, since temperature is the same inside and outside the reactor wall at any time, heat transfer is cancelled and adiabatic behaviour is achieved, even at unsteady state conditions.

Large-scale reactors are aimed at pilot-scale demonstrations. In these devices, the reactor is usually operated for long periods, often with real 'on site' emissions, allowing the collection of valuable data on the control and stability or the possibilities of heat recovery from the reactor [28,55,56,58,137,138].

5.3. Autothermal operation

Reverse flow reactors are integrated regenerative reacting systems. Hence, the heat released by exothermic reactions plays a critical role in the efficiency and the stable operation of the device. Too low heat of reaction results in reactor extinction, the energy released by the reaction not being enough to overcome heat losses. On the contrary, too high heat of reaction results in an accumulation of the excess of heat cycle after cycle, which will result in temperature build-up and damage to the catalyst or the device.

The heat of reaction is, therefore, a critical parameter to consider in the design and testing of reverse flow reactors. In VOC oxidation, it

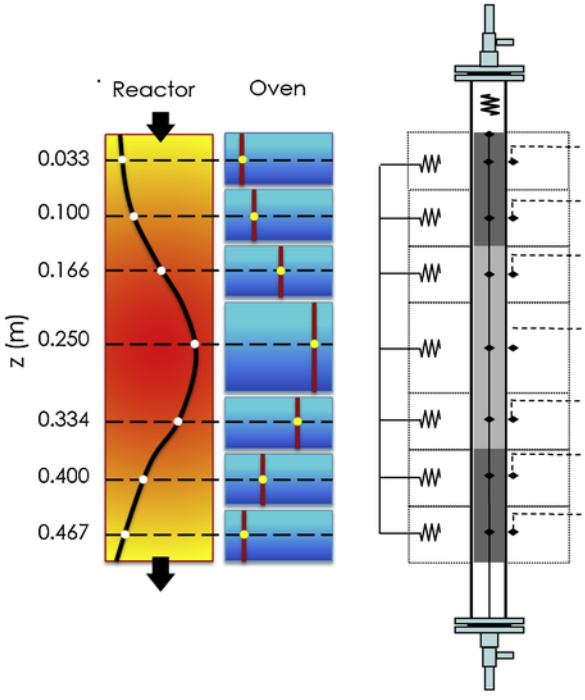

Fig. 4. Sketch of an oven capable of compensating the heat losses and achieving adiabatic behaviour in reverse flow reactors [136].

should be taken into account that each organic compound has a different combustion enthalpy and, hence, the heat released in the reactor for total combustion for the same feed concentration (e.g. mole fraction) may be different. Therefore, it is recommended the use of the adiabatic temperature rise, as a more adequate measurement of reaction enthalpy and feed concentration, when comparing the performance of RFR with different feeds. It should be noted that two reactions of different heat of reaction, but the same adiabatic temperature rise, may exhibit a similar thermal performance in a reverse flow reactor.

The first question in the design of a reverse flow reactor is determining the minimum feed concentration necessary to achieve autothermal operation [139]. The heat storage efficiency (η_{th}) is defined as the ratio of the heat stored in the reactor between cycles (Q_{st}) and the total amount of heat that can be theoretically stored, i.e. the pre-heating heat (Q_{ph}) plus the heat released in the reaction (Q_r).

$$\eta_{th} = \frac{Q_{st}}{Q_{ph} + Q_r}$$

Autothermal operation is possible when the required pre-heating heat is lower than the heat stored in the reactor between cycles. Otherwise, the reactor is unable to pre-heat additional fresh feed and will extinguish. Thus, $Q_{ph} < Q_{st}$ implies that $Q_{ph} < \eta_{th}(Q_{ph} + Q_r)$.

Where $Q_{ph} = mC_{PG}\Delta T_{ph}$ and $Q_r = my_0(-\Delta H_R)/M_w = mC_{PG}\Delta T_{ad}$, resulting in the following expression:

$$\Delta T_{ph} < \eta_{th}\left(\Delta T_{ph} + \Delta T_{ad}\right)$$

By rearranging the previous equation, we obtain that auto-thermal operation is possible if [83,140]:

$$\Delta T_{ad} > \frac{1-\eta_{th}}{\eta_{th}}\Delta T_{ph}$$

i.e. ΔT_{ad} of the feed should be higher than ΔT_{ph} (pre-heating temperature increase) multiplied by a number which is a function of the heat storage efficiency of the reactor.

The thermal efficiency of reverse flow reactors is usually in the range 90–95%, depending on the design of the equipment and the degree of thermal insulation. The pre-heating temperature rise must ensure that the reacting mixture is heated, at least, to a temperature when the reaction can start (i.e. the ignition temperature). For example, the combustion temperature of methane/air mixtures depends of the type of catalyst, e.g. 350 °C for noble metals, 500 °C for metal oxides and 900 °C without catalyst (homogeneous non-catalytic oxidation). Therefore, according to the previous expression and considering a heat storage efficiency of 90%, the minimum adiabatic temperature rise to achieve autothermal operation is 36 °C (0.13% methane) for noble metal catalysts, 53 °C (0.19% methane) for metal oxide catalysts and 97 °C (0.35% methane) without catalyst.

A given feed has an specific value of ΔT_{ad}, and depending on the reactor characteristics (catalyst and thermal efficiency) requires a given value of ΔT_{ph}. Fig. 5 shows the typical operating window for different types of regenerative oxidizers in terms of pre-heating temperature and adiabatic temperature rise/feed. The RCO are divided into two groups: one with 90% heat storage efficiency and metal oxide catalysts (ΔT_{ph} = 500 °C), and a high-efficiency one (Hi-RCO) with 95% heat storage efficiency and precious metal catalysts (ΔT_{ph} = 350 °C).

5.4. Heat extraction

As introduced in the previous section, the adiabatic temperature rise is a key parameter for the evaluation of autothermal operation in reverse flow reactor. However, sometimes the heat released by the reaction and, hence, the adiabatic temperature exceeds a lot the minimum required for autothermal operation:

$$\Delta T_{ad} \gg \frac{1-\eta_{th}}{\eta_{th}}\Delta T_{ph}$$

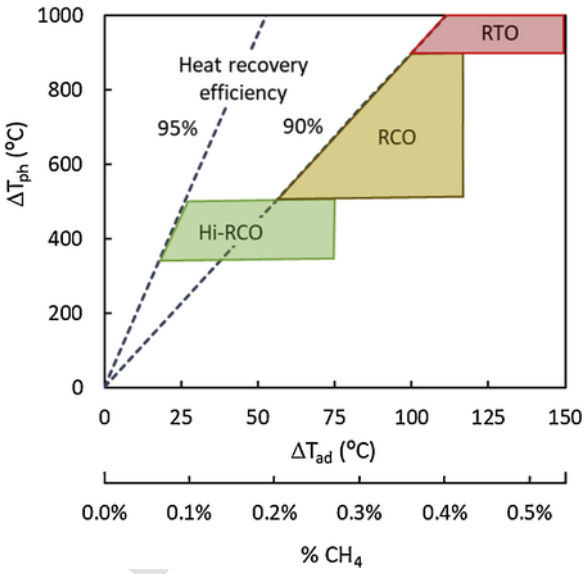

Fig. 5. Operating window of regenerative oxidizers for methane combustion: regenerative thermal oxidizers (RTO) regenerative catalytic oxidizers (RCO) and high-efficiency regenerative catalytic oxidizers (Hi-RCO).

In these situations, there is high risk of suffering from overheating, which may cause damage to the catalyst or the reactor. This issue is overcome by implementing a heat extraction strategy, as presented in Fig. 6. There are two main modes of extracting the excess of heat accumulated in the reactors [56,141–144]: heat exchange and hot gas withdrawal.

The heat exchange is based on the use of a heat exchanger with an external coolant (e.g. water, air, etc.) to decrease the temperature of the reacting gas. The heat exchange in fixed-bed chemical reactors can be accomplished in two ways: multi-tubular reactors and adiabatic beds with inter-stage cooling. In multi-tubular reactors, the catalyst is placed inside the tubes and the cooling media flows through the shell section, or vice versa. Hence, heat exchange takes place along the reactor length. The reaction takes place simultaneously with the exchange of heat and, for this reason, this configuration is recommended when a good temperature control is required. For example, due to a narrow operating window required by the catalyst [145]. However, the main drawback of this type of heat extraction is the generation of asymmetry in the temperature profiles of the reactor, leading to complex dynamic patterns and difficulties in the reactor control [144,146].

Alternatively, in the adiabatic beds with inter-stage cooling, both reaction and heat exchange are carried out separately. In the catalytic beds, the reactor takes place at adiabatic conditions and, hence, the reacting mass is heated due to the heat released by the reaction. For temperature-sensitive catalysts, the reactor must be carefully designed (bed size, feed concentration, etc.) to prevent damaging. The inter-stage cooling consists of heat exchangers where the gas temperature is decreased to drain the excess of heat (Fig. 6a and b). The heat exchangers can be placed in the central open chamber of a typical regenerative oxidizer (as shown in Fig. 6a) or can be external heat exchangers (e.g. a shell and tube or compact heat exchanger) [141,143]. Wang et al. [42] demonstrated the technical feasibility of this heat exchange procedure

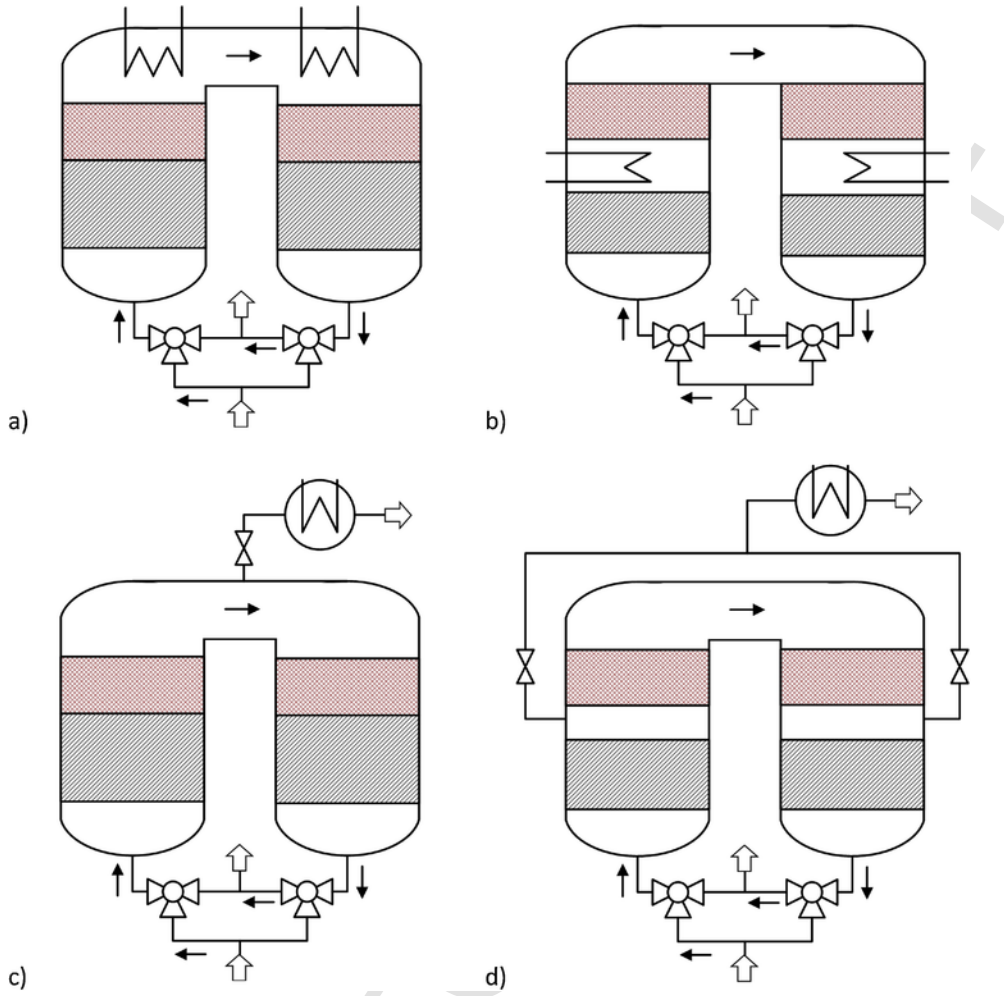

Fig. 6. Modes of heat extraction from reverse flow reactors: heat exchange (a and b) and hot gas withdrawal (c and d). Conventional central heat extraction (a and c) and modified heat extraction to prevent emissions of unreacted compounds [141].

using a spiral heat exchanger refrigerated by water. The amount of heat extracted was adjusted by the temperature difference between the hot gas and the coolant. The temperature profiles, depicted in Fig. 7a, shows that this way of heat extraction produces a marked decrease in temperature, which can affect the behaviour downstream. However, the study concluded that temperature can be effectively regulated using this technique.

The hot gas withdrawal is based on the purge of part of the hot gas from the inside of the reactor, typically the centre of the reactor as depicted in the flowsheet of Fig. 6c. The gas purged is not available to exchange heat with the bed placed downstream and, hence, the amount of sensible heat stored in the bed is lower. As a consequence, in the following cycle, the feed with the pre-heated to a lower temperature. This way, the temperature build-up between cycles is avoided and controlled. Since, the heat is extracted as sensible heat of a gas stream, the amount of heat extracted is easily regulated by adjusting its flow rate. One of the advantages of hot gas withdrawal is that this way of heat extraction does not cause a direct decrease of temperature in the reactor, like those based on heat exchangers. Therefore, the dynamic behaviour of the reverse flow reactor is disturbed to a least extent (for the same amount of energy extracted) [42,56,141].

This mode of heat extraction was recently studied from an experimental point of view by Gosiewski et al. [142], Kushwaha et al. [56] and Li et al. [55,147]. Kushwaha et al. [56] found that the use of an internal heat exchanger more significantly decreased the temperature in the centre of the reactor than hot air withdrawal (Fig. 7b). Li et al. [55] successfully operated a pilot-scale methane RCO with hot gas withdrawal and temperature-control system based on the switching time. They found that hot gas extraction affected the temperature-control system leading to reaction extinction and, for this reason, the set a constant switching time when hot gas withdrawal was practised. Other works address this from a theoretical point of view based on model simulations [147–150].

One of the drawbacks of the technique of hot gas withdrawal when the gas is drained from the centre of the reactor is that the gas may contain an important amount of unreacted compounds. This can be a problem, for example, when using the RFR as a VOC treatment technique, since environmental regulations are strict and VOC conversion must be high. To overcome this issue, the draining point can be moved to the end of the catalytic bed, as shown in Fig. 6d, which ensures a higher conversion [141]. It should be noted that the periodical switch of the flow direction also forces a change in the draining point to the corresponding end of the catalytic bed (which also changes with the flow direction). For this reason, the flowsheet of Fig. 6d incorporates a pair of valves that are alternatively actuated depending of the flow direction.

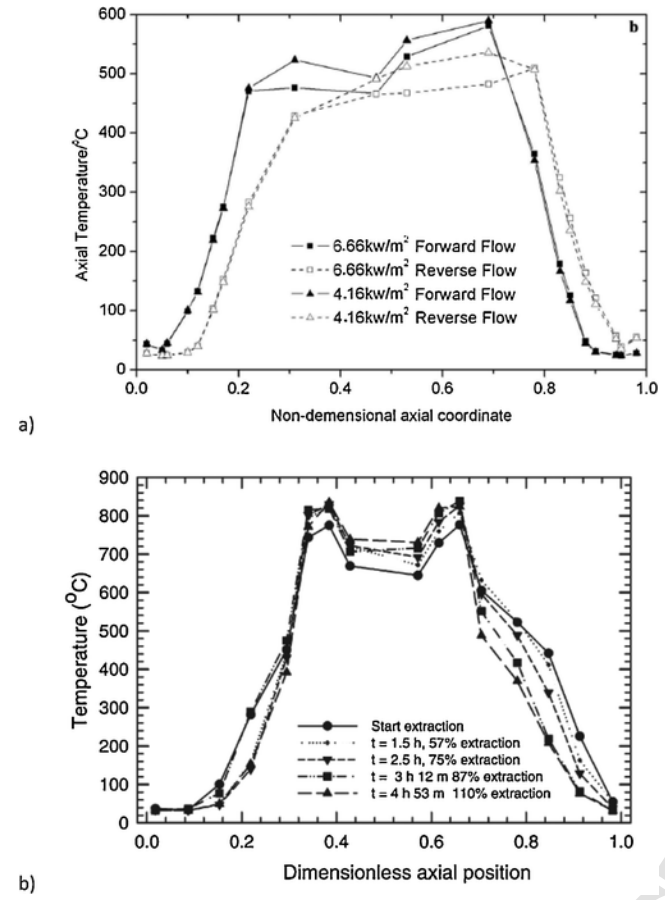

Fig. 7. Comparison of the mode of heat extraction in a lab-scale reverse flow reactor for methane combustion. Evolution of temperature profile for a) Heat exchange (0.4% methane, 0.56 m/s superficial velocity and 120 s switching time) [42] and b) Hot gas withdrawal (0.6% methane, 0.3 m/s superficial velocity and 350 s switching time) [56].

5.5. Integrated adsorption

In the previous sections, the role of reverse flow reactors as integrated thermal regenerative reacting systems has been discussed. Nevertheless, reverse flow reactors also offer the possibility of mass regeneration, based on the adsorption of some compounds.

As presented in section 3.4, one of the applications of reverse flow reactors consists of the abatement of nitrogen oxides by selected catalytic reduction with ammonia. One of the key aspects of this process is the adsorption of the excess of ammonia, preventing the emissions of unreacted ammonia. This mass regeneration can be applied to other systems and integrated with the heat regeneration. Thus, the use of catalysts in regenerative oxidizers is affected by secondary pollutants also present in the emissions, such as water, carbon dioxide or hydrogen sulphide. For example, in coal mine ventilation air, water is present to saturation, and sometimes also carbon dioxide; in landfill and waste water treatment plant emissions, water, carbon dioxide and hydrogen sulphide are common [36,43]. Thus, it is well known that hydrogen sulphide causes catalyst deactivation (poisoning) in precious metal catalysts. On the other hand, water is responsible of inhibition of the catalyst activity (competitive adsorption), resulting in a decrease in reaction rate and hence RFR stability, as demonstrated experimentally [41,43].

Integrated adsorption has been proposed as a way to eliminate the problems caused by these secondary pollutants, without the need of additional expensive pre-treatments [151]. In integrated adsorption, part of the bed at both reactor sides (which are normally occupied by inert material) consists of a solid adsorbent, selected in order to capture the undesired compounds present in the feed (e.g. water or hydrogen sulphide). This way, when the feed reaches the catalyst in the centre of the bed is free of these compounds, and catalyst deactivation/inhibition is avoided. It should be noted that the adsorbent beds in RFR are not a mere guard beds, because the forced unsteady state character of RFR, together with its parabolic temperature profile (high temperature in the centre and low temperature at the reactor sides), makes it possible the self-regeneration of the adsorbent beds. Thus, the feed that enters the first adsorbent bed is cold, so adsorption is favoured. At the same time, the second adsorbent bed, placed on the other side of the reactor (at the reactor exit in this part of the cycle), is being heated by the hot reacted gas that leaves the catalyst bed. This promotes desorption of the undesired compounds adsorbed in the previous semi-cycle (adsorption equilibrium is highly affected by temperature) and, hence, the self-regeneration of the adsorbents is accomplished.

The integrated adsorption concept has been experimentally demonstrated for the catalytic oxidation of methane in lab-scale RFRs. Inhibition caused by water (1.7–2.7%) was avoided using γ -alumina adsorbents [152]. Fig. 8 shows the flowsheet diagram and adsorbed water concentration profiles of an integrated adsorption unit designed for the abatement of ventilation air methane emissions [153]. The case of hydrogen sulphide (100–500 ppm), typically present in emissions from landfills or treatment plants, was also considered using mole sieve 5 A as adsorbent [36].

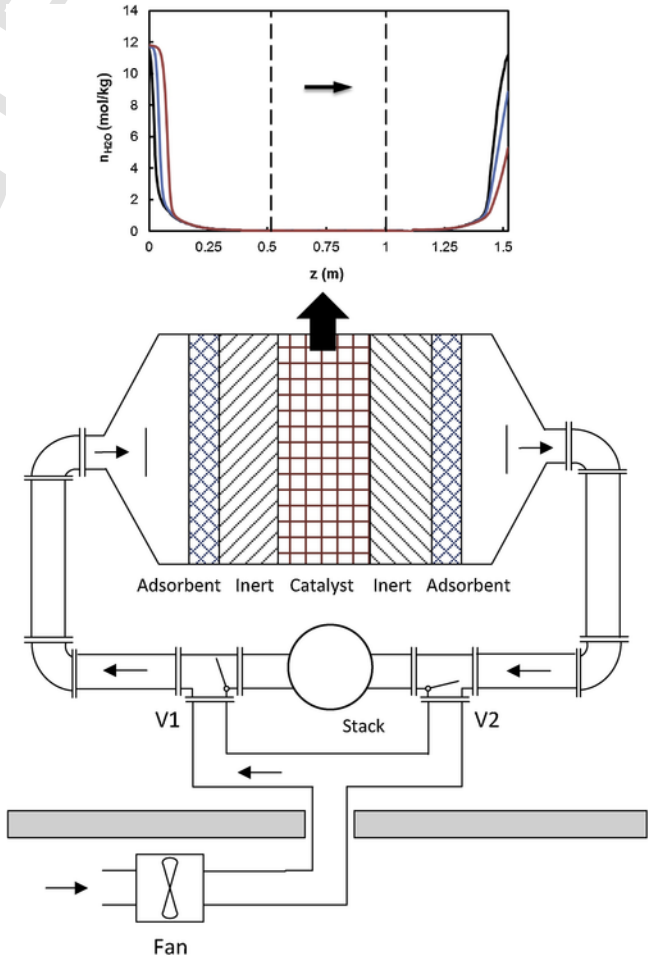

Fig. 8. Sketch of the reverse flow reactor with integrated adsorption [153]. The attached graph shows the profiles of adsorbed water during a cycle: begin (–), middle (–) and end (–) of cycle. The arrow indicates the direction of the flow.

Apart from water and hydrogen sulphide, carbon dioxide is a pollutant commonly found together with methane. As future work, it would be very interesting to capture carbon dioxide (that of the feed, but also the generated in the reaction). This way, the greenhouse effect of methane would be eliminated.

6. Conclusions

The role and applications of reverse flow reactors for the development of sustainable industrial processes have been reviewed. The most important capability of reverse flow reactors is their ability to combine in a single device a chemical reaction with heat or mass regeneration.

The most important application of reverse flow reactors is the oxidation of volatile organic compounds and methane. This application is supported by extensive experimental demonstration at the laboratory and pilot scale. Other applications include the selective catalytic reduction of nitrogen oxides, oxidation of SO_2 to SO_3 or autothermal reforming.

The mathematical model commonly used for reverse flow reactors is the continuous heterogeneous dynamic model, because of being particularly suited to model fast high exothermic or endothermic reactions.

The work also included a revision of the practical considerations to take into account for the research and scale-up of reverse flow reactors. The first thing to consider is the selection of the type of bed, i.e. random packing materials or structured bed. Applications with high flow rates favours the use of monolithic beds, because of the lower pressure drop. In these cases, the decrease in thermal inertia of the bed is compensated with a higher bed length. The autothermal operation and heat extraction opportunities are critical for the economy of the process and for this reason they have been evaluated in detail. Thus, the conditions leading to autothermal operation depend of the heat of reaction, the concentration of reactants and the type of catalyst (the reaction temperature). The excess of heat must be extracted from the reactor to prevent overheating and this can be carried out by different means. According to the experimental works, the hot extraction from the centre of the reactor is able of controlling temperature with low impact in the reactor stability.

Finally, the integrated adsorption concept was introduced. According to this technique, the reverse flow reactor is used to adsorb in the bed some of the compounds. As with heat regeneration, the mass regeneration can be valuable tool when applied to the reactants, products or compounds that reduce the catalyst activity (e.g. water in catalytic oxidation).

Acknowledgements

This project has received funding from the Research Fund for Coal and Steel (EU) under the grant agreement No 754077 (METHENERGY + Project).

References

[1] V. Bukarica, Ž. Tomšić, Energy efficiency policy evaluation by moving from techno-economic towards whole society perspective on energy efficiency market, Renew. Sustain. Energy Rev. 70 (2017) 968–975.
[2] D. Gewald, K. Siokos, S. Karellas, H. Spliethoff, Waste heat recovery from a landfill gas-fired power plant, Renew. Sustain. Energy Rev. 16 (2012) 1779–1789.
[3] G.V.P. Varma, T. Srinivas, Power generation from low temperature heat recovery, Renew. Sustain. Energy Rev. 75 (2017) 402–414.
[4] M. Hasanuzzaman, N.A. Rahim, M. Hosenuzzaman, R. Saidur, I.M. Mahbubul, M.M. Rashid, Energy savings in the combustion based process heating in industrial sector, Renew. Sustain. Energy Rev. 16 (2012) 4527–4536.
[5] Y.S.H. Matros, G.A. Bunimovich, Reverse-flow operation in fixed bed catalytic reactors, Catal. Rev. Sci. Eng. 38 (1996) 1–68.
[6] G. Bunimovich, H. Sapoundjiev, Chapter 18 - periodic flow reversal, in: P.L. Silveston, R.R. Hudgins (Eds.), Periodic Operation of Chemical Reactors,, Butterworth-Heinemann, Oxford, 2013, pp. 495–542.
[7] F.G. Cottrell, in: U. Patents (Ed.), Purifying Gases and Apparatus Therefor, 1938.
[8] A. Zagoruiko, The Reverse-flow Operation of Catalytic Reactors: History and Prospects, 2012.
[9] C.D. Luzi, O.M. Martínez, G.F. Barreto, Autothermal reverse-flow reactors: design and comparison of valve-operated and rotary systems, Chem. Eng. Sci. 148 (2016) 170–181.
[10] E. Muñoz, P. Marín, F.V. Díez, S. Ordóñez, Selective catalytic reduction of NO in a reverse-flow reactor: modelling and experimental validation, Appl. Energy 138 (2015) 183–192.
[11] Y.W. Budhi, A. Jaree, J.H.B.J. Hoebink, J.C. Schouten, Simulation of reverse flow operation for manipulation of catalyst surface coverage in the selective oxidation of ammonia, Chem. Eng. Sci. 59 (2004) 4125–4135.
[12] J. Dunnewijk, H. Bosch, A.B. de Haan, Reverse flow adsorption: integrating the recovery and recycling of homogeneous catalysts, Sep. Purif. Technol. 40 (2004) 317–320.
[13] K.G.W. Hung, D. Papadias, P. Björnbom, M. Anderlund, B. Åkermark, Reverse-flow operation for application of imperfectly immobilized catalysts, Aiche J. 49 (2003) 151–167.
[14] P.L. Silveston, R.R. Hudgins, Periodic Operation of Chemical Reactors, Butterworth-Heinemann, Oxford, 2013.
[15] T. Aida, P.L. Silveston, Cyclic Separating Reactors, Blackwell Publishing Ltd, 2005.
[16] S. Ordóñez, L. Bello, H. Sastre, R. Rosal, F.V. Díez, Kinetics of the deep oxidation of benzene, toluene, n-hexane and their binary mixtures over a platinum on γ-alumina catalyst, Appl. Catal. B 38 (2002) 139–149.
[17] G. Baldissone, D. Fissore, M. Demichela, Catalytic after-treatment of lean VOC-air streams: process intensification vs. plant reliability, Process Safety Environ. Protect. 100 (2016) 208–219.
[18] M.S. Chou, W.H. Cheng, W.S. Lee, Performance characteristics of a regenerative catalytic oxidizer for treating VOC-contaminated airstreams, J. Air Waste Manage. Assoc. 50 (2000) 2112–2119.
[19] W.H. Cheng, M.S. Chou, W.S. Lee, B.J. Huang, Applications of low-temperature regenerative thermal oxidizers to treat volatile organic compounds, J. Environ. Eng. 128 (2002) 313–319.
[20] F. Cunill, L. Van De Beld, K.R. Westerterp, Catalytic combustion of very lean mixtures in a reverse flow reactor using an internal electrical heater, Ind. Eng. Chem. Res. 36 (1997) 4198–4206.
[21] P. Marín, S. Ordóñez, F.V. Díez, Combustion of toluene-hexane binary mixtures in a reverse flow catalytic reactor, Chem. Eng. Sci. 63 (2008) 5003–5009.
[22] B.T. Moshe, E. Alajem, R. Gal, M. Sheintuch, Flow-rate effects in flow-reversal reactors: experiments, simulations and approximations, Chem. Eng. Sci. 58 (2003) 1135–1146.
[23] A.Y. Madai, M. Sheintuch, Demonstration of loop reactor operation, Aiche J. 54 (2008) 2413–2422.
[24] K. Ramdani, R. Pontier, D. Schweich, Reverse flow reactor at short switching periods for VOC combustion, Chem. Eng. Sci. 56 (2001) 1531–1539.
[25] D. Edouard, H. Hammouri, X.G. Zhou, Control of a reverse flow reactor for VOC combustion, Chem. Eng. Sci. 60 (2005) 1661–1672.
[26] P. Tunå, F. Bauer, C. Hulteberg, L. Malek, Regenerative reverse-flow reactor system for cracking of producer gas tars, Biomass Convers. Biorefinery 4 (2014) 43–51.
[27] G. Chen, Y. Chi, C. Pan, J. Yan, M. Ni, Methane-benzene binary mixture destruction in a reverse flow catalytic reactor, J. Mater. Cycles Waste Manag. 13 (2011) 219–224.
[28] J.C. Lou, S.W. Huang, Treating isopropyl alcohol by a regenerative catalytic oxidizer, Sep. Purif. Technol. 62 (2008) 71–78.
[29] S.W. Huang, J.C. Lou, Y.C. Lin, Treatment of VOCs with molecular sieve catalysts in regenerative catalytic oxidizer, J. Hazard. Mater. 183 (2010) 641–647.
[30] S. Vigneron, P. Deprelle, J. Hermia, Comparison of precious metals and base metal oxides for catalytic deep oxidation of volatile organic compounds from coating plants: test results on an industrial pilot scale incinerator, Catal. Today 27 (1996) 229–236.
[31] R.E. Hayes, M.D. Checkel, Reversing flow catalytic converter for a natural gas/diesel dual fuel engine, Chem. Eng. Sci. 56 (2001) 2641–2658.
[32] B. Liu, M.D. Checkel, R.E. Hayes, Experimental study of a reverse flow catalytic converter for a dual fuel engine, Can. J. Chem. Eng. 79 (2001) 491–506.
[33] L.F. Liotta, Catalytic oxidation of volatile organic compounds on supported noble metals, Appl. Catal. B 100 (2010) 403–412.
[34] A. Zagoruiko, Modeling of reverse-flow reactor for VOC incineration with account of reversible adsorption: the way to minimize the negative influence of desorption phenomena, Int. J. Chem. React. Eng. 6 (2008).
[35] G. Myhre, D. Shindell, F.-M. Bréon, W. Collins, J. Fuglestvedt, J. Huang, D. Koch, J.-F. Lamarque, D. Lee, B. Mendoza, T. Nakajima, A. Robock, G. Stephens, T. Takemura, H. Zhang, Anthropogenic and natural radiative forcing, climate change 2013: the physical science basis, 5th Assessment Report of the Intergovernmental Panel on Climate Change (IPCC), Cambridge University Press, Cambridge, United Kingdom and New York, NY, USA, 2013.
[36] C. Urbani, P. Marín, F.V. Díez, S. Ordóñez, Catalytic combustion of sulphur-containing methane lean emissions in a reverse-flow reactor with integrated adsorption, Chem. Eng. J. 285 (2016) 39–48.
[37] I. Karakurt, G. Aydin, K. Aydiner, Sources and mitigation of methane emissions by sectors: a critical review, Renew. Energy 39 (2012) 40–48.
[38] I. Karakurt, G. Aydin, K. Aydiner, Mine ventilation air methane as a sustainable energy source, Renew. Sustain. Energy Rev. 15 (2011) 1042–1049.

[39] S. Su, X. Yu, Progress in developing an innovative lean burn catalytic turbine technology for fugitive methane mitigation and utilization, Front. Energy 5 (2011) 229.

[40] P. Marín, S. Ordóñez, F.V. Díez, Systematic study of the performance of a reverse flow reactor for the treatment of lean hydrocarbon emissions, J. Chem. Technol. Biotechnol. 84 (2009) 1292–1302.

[41] W. Liang, H. Liu, J. Li, Ventilation air methane combustion in a flow reversal catalytic reactor: effect of catalyst, reactor properties and humidity, Fresenius Environ. Bull. 26 (2017) 2302–2313.

[42] S. Wang, D. Gao, S. Wang, Steady and transient characteristics of catalytic flow reverse reactor integrated with central heat exchanger, Ind. Eng. Chem. Res. 53 (2014) 12644–12654.

[43] J. Fernández, P. Marín, F.V. Díez, S. Ordóñez, Coal mine ventilation air methane combustion in a catalytic reverse flow reactor: influence of emission humidity, Fuel Process. Technol. 133 (2015) 202–209.

[44] C.R. Thompson, P. Marín, F.V. Díez, S. Ordóñez, Evaluation of the use of ceramic foams as catalyst supports for reverse-flow combustors, Chem. Eng. J. 221 (2013) 44–54.

[45] G. Chen, Y. Chi, J.H. Yan, M.J. Ni, Effect of periodic variation of the inlet concentration on the performance of reverse flow reactors, Ind. Eng. Chem. Res. 50 (2011) 5448–5458.

[46] P. Marín, S. Ordóñez, F.V. Díez, Monoliths as suitable catalysts for reverse-flow combustors: modeling and experimental validation, Aiche J. 56 (2010) 3162–3173.

[47] M.A.G. Hevia, S. Ordóñez, F.V. Díez, D. Fissore, A.A. Barresi, Design and testing of a control system for reverse-flow catalytic afterburners, Aiche J. 51 (2005) 3020–3027.

[48] J. Chaouki, C. Guy, C. Sapundzhiev, D. Kusohorsky, D. Klvana, Combustion of methane in a cyclic catalytic reactor, Ind. Eng. Chem. Res. 33 (1994) 2957–2963.

[49] P. Forzatti, G. Groppi, Catalytic combustion for the production of energy, Catal. Today 54 (1999) 165–180.

[50] T.V. Choudhary, S. Banerjee, V.R. Choudhary, Catalysts for combustion of methane and lower alkanes, Appl. Catal. A Gen. 234 (2002) 1–23.

[51] R.F. Hicks, H. Qi, M.L. Young, R.G. Lee, Effect of catalyst structure on methane oxidation over palladium on alumina, J. Catal. 122 (1990) 295–306.

[52] K.-i. Fujimoto, F.H. Ribeiro, M. Avalos-Borja, E. Iglesia, Structure and reactivity of PdOx/ZrO2Catalysts for methane oxidation at low temperatures, J. Catal. 179 (1998) 431–442.

[53] A.K. Neyestanaki, L.E. Lindfors, Catalytic combustion of propane and natural gas over silica-fibre supported catalysts, Combust. Sci. Technol. 110-111 (1995) 303–320.

[54] R.J. Farrauto, M.C. Hobson, T. Kennelly, E.M. Waterman, Catalytic chemistry of supported palladium for combustion of methane, Appl. Catal. A Gen. 81 (1992) 227–237.

[55] Z. Li, Z. Wu, Z. Qin, H. Zhu, J. Wu, R. Wang, L. Lei, J. Chen, M. Dong, W. Fan, J. Wang, Demonstration of mitigation and utilization of ventilation air methane in a pilot scale catalytic reverse flow reactor, Fuel Process. Technol. 160 (2017) 102–108.

[56] A. Kushwaha, M. Poirier, R.E. Hayes, H. Sapoundjiev, Heat extraction from a flow reversal reactor in lean methane combustion, Chem. Eng. Res. Des. 83 (2005) 205–213.

[57] A. Kushwaha, M. Poirier, H. Sapoundjiev, R.E. Hayes, Effect of reactor internal properties on the performance of a flow reversal catalytic reactor for methane combustion, Chem. Eng. Sci. 59 (2004) 4081–4093.

[58] S. Salomons, R.E. Hayes, M. Poirier, H. Sapoundjiev, Flow reversal reactor for the catalytic combustion of lean methane mixtures, Catal. Today 83 (2003) 59–69.

[59] P. Marín, S. Ordóñez, F.V. Díez, Simplified design methods of reverse flow catalytic combustors for the treatment of lean hydrocarbon-air mixtures, Chem. Eng. Process. Process. Intensif. 48 (2009) 229–238.

[60] B. Lan, Y.R. Li, Numerical study on thermal oxidation of lean coal mine methane in a thermal flow-reversal reactor, Chem. Eng. J. 351 (2018) 922–929.

[61] Z. Li, Y. Liu, J. Han, Z. Wang, Numerical study on heat distribution and transfer characteristics of a manifold in a coal mine VAM TFRR oxidation bed, Open Mech. Eng. J. 9 (2015) 687–696.

[62] B. Zheng, Y. Liu, P. Sun, J. Meng, R. Liu, Dehydrogenation characteristics of lean methane in a thermal reverse-flow reactor, Int. J. Hydrogen Energy (2018).

[63] Z. Li, Y. Liu, Z. Wang, Experimental study on thennal oxidation of ultra-low concentration methane in a non-catalytic reverse-flow reactor, Bulgar. Chem. Commun. 48 (2016) 793–797.

[64] X.N. Qi, Y.Q. Liu, H.Q. Xu, Z.Y. Liu, R.X. Liu, Modeling thermal oxidation of coal mine methane in a non-catalytic reverse-flow reactor, Strojniski Vestnik J. Mech. Eng. 60 (2014) 495–505.

[65] G.G. Grozev, C.G. Sapundzhiev, D.G. Elenkov, UNSTEADY-STATE SO2 oxidation - practical results, Ind. Eng. Chem. Res. 33 (1994) 2248–2250.

[66] R. Hong, X. Li, H. Li, W. Yuan, Modeling and simulation of SO2 oxidation in a fixed-bed reactor with periodic flow reversal, Catal. Today 38 (1997) 47–58.

[67] G.A. Bunimovich, N.V. Vernikovskaya, V.O. Strots, B.S. Balzhinimaev, Y.S. Matros, SO2 oxidation in a reverse-flow reactor: influence of a vanadium catalyst dynamic properties, Chem. Eng. Sci. 50 (1995) 565–580.

[68] K. Gosiewski, Dynamic modelling of industrial SO2 oxidation reactors. Part II. Model of a reverse-flow reactor, Chem. Eng. Process. 32 (1993) 233–244.

[69] W.D. Xiao, H. Wang, W.K. Yuan, Unsteady-state SO < inf > 2 < /inf > converters with inter-stage heat removal, Chem. Eng. Sci. 54 (1999) 4629–4638.

[70] W.D. Xiao, H. Wang, W.K. Yuan, Practical studies of the commercial flow-reversed SO < inf > 2 < /inf > converter, Chem. Eng. Sci. 54 (1999) 4645–4652.

[71] W.D. Xiao, H. Wang, W.K. Yuan, A novel unsteady-state SO < inf > 2 < /inf > converter for relatively concentrated SO < inf > 2 < /inf > gases, Chem. Eng. Sci. 54 (1999) 1333–1338.

[72] A.N. Zagoruiko, S.V. Vanag, Reverse-flow reactor concept for combined SO2 and co-oxidation in smelter off-gases, Chem. Eng. J. 238 (2014) 86–92.

[73] R.M. Heck, Catalytic abatement of nitrogen oxides–stationary applications, Catal. Today 53 (1999) 519–523.

[74] S. Roy, M.S. Hegde, G. Madras, Catalysis for NOx abatement, Appl. Energy 86 (2009) 2283–2297.

[75] E. Tronconi, I. Nova, C. Ciardelli, D. Chatterjee, B. Brandl-Konrad, T. Burkhardt, Modelling of an SCR catalytic converter for diesel exhaust after treatment: dynamic effects at low temperature, Catal. Today 105 (2005) 529–536.

[76] D.W. Agar, W. Ruppel, Extended reactor concept for dynamic DeNOx design, Chem. Eng. Sci. 43 (1988) 2073–2078.

[77] A.S. Noskov, L.N. Bobrova, Y.S. Matros, Reverse-process for NOx - off gases decontamination, Catal. Today 17 (1993) 293–300.

[78] E.S. Borisova, A.S. Noskov, L.N. Bobrova, Effect of unsteady-state catalyst surface on the SCR-process, Catal. Today 38 (1997) 97–105.

[79] J.D. Snyder, B. Subramaniam, Numerical simulation of a reverse-flow NOx-SCR reactor with side-stream ammonia addition, Chem. Eng. Sci. 53 (1998) 727–734.

[80] Y.W. Budhi, J. Hoebink, J.C. Schouten, Reverse flow operation with reactor side feeding: analysis, modeling, and simulation, Ind. Eng. Chem. Res. 43 (2004) 6955–6963.

[81] Y.W. Budhi, A. Jaree, J. Hoebink, J.C. Schouten, Simulation of reverse flow operation for manipulation of catalyst surface coverage in the selective oxidation of ammonia, Chem. Eng. Sci. 59 (2004) 4125–4135.

[82] D. Fissore, A.A. Barresi, C.C. Botar-Jid, NOx removal in forced unsteady-state chromatographic reactors, Chem. Eng. Sci. 61 (2006) 3409–3414.

[83] P. Marín, D. Fissore, A.A. Barresi, S. Ordóñez, Simulation of an industrial-scale process for the SCR of NOx based on the loop reactor concept, Chem. Eng. Process. Process. Intensif. 48 (2009) 311–320.

[84] C.C. Botar-Jid, P.S. Agachi, D. Fissore, Comparison of reverse flow and counter-current reactors in the case of selective catalytic reduction of NOx, Comput. Chem. Eng. 33 (2009) 782–787.

[85] X. Chen, C. Li, P.L. Silveston, Modeling of a reverse flow reactor for methanol synthesis, Chin. J. Chem. Eng. 11 (2003) 9–14.

[86] S.A. Velardi, A.A. Barresi, Methanol synthesis in a forced unsteady-state reactor network, Chem. Eng. Sci. 57 (2002) 2995–3004.

[87] K.M.V. Bussche, S.N. Neophytides, I.A. Zolotarskii, G.F. Froment, Modelling and simulation of the reversed flow operation of a fixed-bed reactor for methanol synthesis, Chem. Eng. Sci. 48 (1993) 3335–3345.

[88] S.G. Neophytides, G.F. Froment, A bench scale study of reversed flow methanol synthesis, Ind. Eng. Chem. Res. 31 (1992) 1583–1589.

[89] T. Egyházy, J. Kovács, J. Scholtz, Experimental study of flow reversal ammonia synthesis, Chem. Eng. Technol. 21 (1998) 967–974.

[90] A.P. Gerasev, Y.S. Matros, Unstationary method of ammonia synthesis, Teoreticheskie Osnovy Khimicheskoi Tekhnologii 25 (1991) 821–827.

[91] P. Marín, S. Ordóñez, F.V. Díez, Performance of reverse flow monolithic reactor for water-gas shift reaction, Catal. Today 147 (2009) S185–S190.

[92] K.V. Dobrego, N.N. Gnezdilov, S.H. Lee, H.K. Choi, Methane partial oxidation reverse flow reactor scale up and optimization, Int. J. Hydrogen Energy 33 (2008) 5501–5509.

[93] K.V. Dobrego, N.N. Gnezdilov, S.H. Lee, H.K. Choi, Partial oxidation of methane in a reverse flow porous media reactor. Water admixing optimization, Int. J. Hydrogen Energy 33 (2008) 5535–5544.

[94] D. Fissore, A.A. Barresi, G. Baldi, Synthesis gas production in a forced unsteady-state reactor network, Ind. Eng. Chem. Res. 42 (2003) 2489–2495.

[95] K. Gosiewski, Simulations of non-stationary reactors for the catalytic conversion of methane to synthesis gas, Chem. Eng. Sci. 56 (2001) 1501–1510.

[96] K. Gosiewski, U. Bartmann, M. Moszczyński, L. Mleczko, Effect of the intraparticle mass transport limitations on temperature profiles and catalytic performance of the reverse-flow reactor for the partial oxidation of methane to synthesis gas, Chem. Eng. Sci. 54 (1999) 4589–4602.

[97] N.S. Kaisare, J.H. Lee, A.G. Fedorov, Operability analysis and design of a reverse-flow microreactor for hydrogen generation via methane partial oxidation, Ind. Eng. Chem. Res. 44 (2005) 8323–8333.

[98] N.S. Kaisare, J.H. Lee, A.G. Fedorov, Hydrogen generation in a reverse-flow microreactor: 1. Model formulation and scaling, AIChE J. 51 (2005) 2254–2264.

[99] N.S. Kaisare, J.H. Lee, A.G. Fedorov, Hydrogen generation in a reverse-flow microreactor: 2. Simulation and analysis, AIChE J. 51 (2005) 2265–2272.

[100] T. Liu, H. Temur, G. Veser, Autothermal reforming of methane in a reverse-flow reactor,, Chem. Eng. Technol. 32 (2009) 1358–1366.

[101] A. Mitri, D. Neumann, T. Liu, G. Veser, Reverse-flow reactor operation and catalyst deactivation during high-temperature catalytic partial oxidation, Chem. Eng. Sci. 59 (2004) 5527–5534.

[102] D. Neumann, G. Veser, Catalytic partial oxidation of methane in a high-temperature reverse-flow reactor, Aiche J. 51 (2005) 210–223.

[103] R. Quinta Ferreira, C. Almeida Costa, S. Masetti, Reverse-flow reactor for a selective oxidation process, Chem. Eng. Sci. 54 (1999) 4615–4627.

[104] M. Simeone, L. Menna, L. Salemme, C. Allouis, Temperature evolution on Rh/Al2O3 catalyst during partial oxidation of methane in a reverse flow reactor, Exp. Therm. Fluid Sci. 34 (2010) 381–386.

[105] M. Simeone, L. Salemme, C. Allouis, G. Volpicelli, Temperature profile in a reverse flow reactor for catalytic partial oxidation of methane by fast IR imaging, Aiche J. 54 (2008) 2689–2698.
[106] M. Simeone, L. Salemme, L. Menna, , Methane autothermal reforming in a reverse flow reactor on Rh/Al 2O 3 catalyst, Int. J. Hydrogen Energy 37 (2012) 9049–9057.
[107] J. Smit, G.J. Bekink, M. Van Sint Annaland, J.A.M. Kuipers, A reverse flow catalytic membrane reactor for the production of syngas: an experimental study, Int. J. Chem. React. Eng. 3 (2005).
[108] J. Smit, G.J. Bekink, M. van Sint Annaland, J.A.M. Kuipers, Experimental demonstration of the reverse flow catalytic membrane reactor concept for energy efficient syngas production. Part 1: influence of operating conditions, Chem. Eng. Sci. 62 (2007) 1239–1250.
[109] J. Smit, G.J. Bekink, M. van Sint Annaland, J.A.M. Kuipers, Experimental demonstration of the reverse flow catalytic membrane reactor concept for energy efficient syngas production. Part 2:. Model development, Chem. Eng. Sci. 62 (2007) 1251–1262.
[110] J. Smit, M. Van Sint Annaland, J.A.M. Kuipers, Modelling of a reverse flow catalytic membrane reactor for the partial oxidation of methane, Int. J. Chem. React. Eng. 1 (2002).
[111] J. Smit, M. Van Sint Annaland, J.A.M. Kuipers, Feasibility study of a reverse flow catalytic membrane reactor with porous membranes for the production of syngas,, Chem. Eng. Sci. 60 (2005) 6971–6982.
[112] P. Tuna, H. Svensson, J. Brandin, Modelling of a reverse-flow partial oxidation reactor for synthesis gas production from gasifier product gas, J. Comput. Methods Sci. Eng. 15 (2015) 593–604.
[113] B. Glöckler, G. Kolios, C. Tellaeche, U. Nieken, A heat-integrated reverse-flow reactor concept for endothermic high-temperature, Chem. Eng. Technol. 32 (2009) 1339–1347.
[114] T.P. Tiemersma, T. Kolkman, J.A.M. Kuipers, M.V. Annaland, A novel autothermal reactor concept for thermal coupling of the exothermic oxidative coupling and endothermic steam reforming of methane, Chem. Eng. J. 203 (2012) 223–230.
[115] B. Glöckler, H. Dieter, G. Eigenberger, U. Nieken, Efficient reheating of a reverse-flow reformer-An experimental study, Chem. Eng. Sci. 62 (2007) 5638–5643.
[116] B. Glöckler, A. Gritsch, A. Morillo, G. Kolios, G. Eigenberger, Autothermal reactor concepts for endothermic fixed-bed reactions, Chem. Eng. Res. Des. 82 (2004) 148–159.
[117] B. Glöckler, G. Kolios, G. Eigenberger, Analysis of a novel reverse-flow reactor concept for autothermal methane steam reforming, Chem. Eng. Sci. 58 (2003) 593–601.
[118] A.N. Zagoruiko, Y.S. Matros, Mathematical modelling of Claus reactors undergoing sulfur condensation and evaporation, Chem. Eng. J. 87 (2002) 73–88.
[119] K. Nalpantidis, F. Platte, D.W. Agar, S. Turek, Elucidation of hybrid N2O decomposition using axially structured catalyst in reverse flow reactor, Chem. Eng. Sci. 61 (2006) 3176–3185.
[120] G.F. Froment, K.B. Bischoff, J.D. Wilde, Chemical Reactor Analysis and Design, 3rd ed., John Wiley and Sons, 2011.
[121] C.C. Botar-Jid, Y. Avramenko, A. Kraslawski, P.S. Agachi, Case-based selection of a model of a reverse flow reactor, Chem. Eng. Process.: Process Intensif. 49 (2010) 74–83.
[122] G. Kolios, D. Luss, R. Garg, G. Viswanathan, Efficient computation of periodic state of cyclic fixed-bed processes, Chem. Eng. Sci. 101 (2013) 90–98.
[123] B.Avd. Rotten, S.M.V. Lunel, A. Bliek, Efficient simulation of periodically forced reactors with radial gradients, Chem. Eng. Sci. 61 (2006) 6981–6994.
[124] B. Liu, R.E. Hayes, Y. Yi, J. Mmbaga, M.D. Checkel, M. Zheng, Three dimensional modelling of methane ignition in a reverse flow catalytic converter, Comput. Chem. Eng. 31 (2007) 292–306.
[125] G. Groppi, E. Tronconi, P. Forzatti, Mathematical models of catalytic combustors,, Catal. Rev. 41 (1999) 227–254.
[126] P. Marín, M.A.G. Hevia, S. Ordóñez, F.V. Díez, Combustion of methane lean mixtures in reverse flow reactors: comparison between packed and structured catalyst beds, Catal. Today 105 (2005) 701–708.
[127] G. Kolios, J. Frauhammer, G. Eigenberger, Autothermal fixed-bed reactor concepts,, Chem. Eng. Sci. 55 (2000) 5945–5967.
[128] P. Marín, F.V. Díez, S. Ordóñez, A new method for controlling the ignition state of a regenerative combustor using a heat storage device, Appl. Energy 116 (2014) 322–332.
[129] R.B. Bird, W.E. Stewart, E.N. Lightfoot, , Transport Phenomena, 2nd ed., John Wiley, New York, 2002.
[130] T. Boger, A.K. Heibel, C.M. Sorensen, Monolithic catalysts for the chemical industry, Ind. Eng. Chem. Res. 43 (2004) 4602–4611.
[131] K. Gosiewski, Y.S. Matros, K. Warmuzinski, M. Jaschik, M. Tanczyk, Homogeneous vs. Catalytic combustion of lean methane-air mixtures in reverse-flow reactors, Chem. Eng. Sci. 63 (2008) 5010–5019.
[132] Y. Wang, C. Man, D. Che, Catalytic combustion of ventilation air methane in a reverse-flow reactor, Energy Fuels 24 (2010) 4841–4848.
[133] M.A.G. Hevia, S. Ordóñez, F.V. Díez, Effect of the catalyst properties on the performance of a reverse flow reactor for methane combustion in lean mixtures, Chem. Eng. J. 129 (2007) 1–10.
[134] M.A.G. Hevia, S. Ordóñez, F.V. Díez, Effect of wall properties on the behavior of bench-scale reverse flow reactors, Aiche J. 52 (2006) 3203–3209.
[135] D. Fissore, A.A. Barresi, G. Baldi, M.A.G. Hevia, S. Ordóñez, F.V. Dí́ez, Design and testing of small-scale unsteady-state afterburners and reactors, Aiche J. 51 (2005) 1654–1664.
[136] P. Marín, S. Ordóñez, F.V. Díez, Rational design of heating elements using CFD: application to a bench-scale adiabatic reactor, Comput. Chem. Eng. 35 (2011) 2326–2333.
[137] J.L. Nijdam, C.W.M. Van Der Geld, Experiments with a large-scale reverse flow reactor, Chem. Eng. Sci. 52 (1997) 2729–2741.
[138] Y.S. Matros, Performance of catalytic processes under unsteady conditions, Chem. Eng. Sci. 45 (1990) 2097–2102.
[139] A.Y. Madai, O. Nekhamkina, M. Sheintuch, What is the leanest stream to sustain a nonadiabatic loop reactor: analysis and methane combustion experiments, Aiche J. 63 (2017) 2030–2042.
[140] A.A. Barresi, G. Baldi, D. Fissore, Forced unsteady-state reactors as efficient devices for integrated processes: case histories and new perspectives, Ind. Eng. Chem. Res. 46 (2007) 8693–8700.
[141] P. Marín, S. Ordóñez, F.V. Díez, Procedures for heat recovery in the catalytic combustion of lean methane-air mixtures in a reverse flow reactor, Chemical, Eng. J. 147 (2009) 356–365.
[142] K. Gosiewski, A. Pawlaczyk, M. Jaschik, Energy recovery from ventilation air methane via reverse-flow reactors, Energy 92 (2015) 13–23.
[143] K. Gosiewski, K. Warmuzinski, Effect of the mode of heat withdrawal on the asymmetry of temperature profiles in reverse-flow reactors. Catalytic combustion of methane as a test case,, Chem. Eng. Sci. 62 (2007) 2679–2689.
[144] J. Khinast, A. Gurumoorthy, D. Luss, D. Luss, Complex dynamic features of a cooled reverse-flow reactor,, Aiche J. 44 (1998) 1128–1139.
[145] K. Gosiewski, R. Sztaba, M. Moszczyński, Studies of multitubular reactors with internal heat recovery. Experiments with SO2 oxidation, Chem. Eng. Process.: Process Intensif. 35 (1996) 75–85.
[146] J. Khinast, D. Luss, Mapping regions with different bifurcation diagrams of a reverse-flow reactor,, Aiche J. 43 (1997) 2034–2044.
[147] Z. Li, Z. Qin, Y. Zhang, Z. Wu, H. Wang, S. Li, R. Shi, M. Dong, W. Fan, J. Wang, A control strategy of flow reversal with hot gas withdrawal for heat recovery and its application in mitigation and utilization of ventilation air methane in a reverse flow reactor, Chem. Eng. J. 228 (2013) 243–255.
[148] Z. Jia, R.E. Hayes, An efficient computational scheme for building operating maps for a flow reversal reactor, Chem. Eng. Sci. 134 (2015) 423–432.
[149] Y. Zhu, G. Chen, X. Li, G. Yang, Resonance response of reverse flow reactors: a numerical simulation, industrial and engineering, Chem. Res. 54 (2015) 5885–5893.
[150] Z. Li, Z. Qin, Z. Wu, S. Li, Y. Zhang, M. Dong, W. Fan, J. Wang, Fuzzy logic control of a reverse flow reactor for catalytic oxidation of ventilation air methane, Control Eng. Pract. 25 (2014) 112–122.
[151] A.N.R. Bos, J.P. Lange, G. Kabra, A novel reverse flow reactor with integrated separation, Chem. Eng. Sci. 62 (2007) 5661–5662.
[152] J. Fernández, P. Marín, F.V. Díez, S. Ordóñez, Experimental demonstration and modeling of an adsorption-enhanced reverse flow reactor for the catalytic combustion of coal mine ventilation air methane, Chem. Eng. J. 279 (2015) 198–206.
[153] J. Fernández, P. Marín, F.V. Díez, S. Ordóñez, Combustion of coal mine ventilation air methane in a regenerative combustor with integrated adsorption: reactor design and optimization, Appl. Therm. Eng. 102 (2016) 167–175.
[154] P.L. Silveston, R.R. Hudgins, S. Bogdashev, N. Vernijakovskaja, Y.S. Matros, Modelling of a periodically operating packed-bed SO2 oxidation reactor at high conversion, Chem. Eng. Sci. 49 (1994) 335–341.
[155] H.X. Wu, S.Z. Zhang, C.Y. Li, Study of unsteady-state catalytic oxidation of sulfur dioxide by periodic flow reversal, Can. J. Chem. Eng. 74 (1996) 766–771.
[156] J. Kovacs, T. Egyhazy, Selective Catalytic Reduction of NOx by NH3 in an Adiabatic Reverse Flow Reactor, 1998.
[157] C.C. Botar-Jid, P.S. Agachi, D. Fissore, Comparison of reverse flow and counter-current reactors in the case of selective catalytic reduction of NOx, Comput. Chem. Eng. 33 (2009) 782–787.
[158] M. Galle, D.W. Agar, O. Watzenberger, Thermal N2O decomposition in regenerative heat exchanger reactors, Chem. Eng. Sci. 56 (2001) 1587–1595.
[159] M.S. Chou, C.M. Hei, Y.W. Huang, Regenerative thermal oxidation of airborne N,N-dimethylformamide and its associated nitrogen oxides formation characteristics, J. Air Waste Manage. Assoc. 57 (2007) 991–999.
[160] L. Van De Beld, K.R. Westerterp, Air Purification in a Reverse-Flow Reactor: Model Simulations vs. Experiments, Aiche J. 42 (1996) 1139–1148.
[161] B. van de Beld, R.A. Borman, O.R. Derkx, B.A.A. van Woezik, K.R. Westerterp, , Removal of volatile organic compounds from polluted air in a reverse flow reactor: an experimental study, Ind. Eng. Chem. Res. 33 (1994) 2946–2956.
[162] P. Marín, W. Ho, S. Ordóñez, F.V. Díez, Demonstration of a control system for combustion of lean hydrocarbon emissions in a reverse flow reactor, Chem. Eng. Sci. 65 (2010) 54–59.
[163] F. Aubé, H. Sapoundjiev, Mathematical model and numerical simulations of catalytic flow reversal reactors for industrial applications, Comput. Chem. Eng. 24 (2000) 2623–2632.